

Controlling Collective Phenomena by Engineering the Quantum State of Force Carriers: The Case of Photon-Mediated Superconductivity and its Criticality

Ahana Chakraborty^{1,2,*} and Francesco Piazza^{2,†}

¹*Department of Physics and Astronomy, Center for Materials Theory, Rutgers University, Piscataway, NJ 08854, USA*

²*Max Planck Institute for the Physics of Complex Systems, Nöthnitzer Str. 38, 01187, Dresden, Germany.*

(Dated: July 18, 2022)

How are the scattering between the constituents of matter and the resulting collective phenomena affected by preparing the force carriers in different quantum states? This question has become experimentally relevant in a specific non-relativistic version of QED implemented within materials, where standard techniques of quantum optics are available for the preparation of desired quantum states of the carrier photon. We develop the necessary non-equilibrium approach for computing the vertex function and find that, in addition to the energy and momentum structure of the scattering, a further structure emerges which reflects the Hilbert-space distribution of the carrier quantum state. This emergent structure becomes non-trivial for non-Gaussian quantum states of the force carrier, and can dramatically affect interactions and collective phenomena. As a first application, we show that by preparing photons in pure Fock states one can enhance pair correlations, and even control the criticality and universality class of the superconducting phase transition by the choice of the number of photons. Our results also reveal that the thermal mixture of Fock states regularises the strong pair correlations present in each of its components, yielding the standard Bardeen-Cooper-Schrieffer criticality.

I. INTRODUCTION

Interactions between the constituents of matter are, at the fundamental level, always described in terms of force carriers. In the standard model of particle physics, these carriers (or mediators) are gauge Bosons, the most commonly known being the photon, which mediates the interaction between electric charges within quantum electrodynamics (QED).

The nature of the carrier controls the nature of the interactions between the fermionic constituents of matter. For instance, the mass, charge, or spin of the gauge Bosons determine the properties of the force they mediate. Within the full quantum mechanical description, the gauge Bosons are excitations of a field. Therefore, in addition to the above single particle properties, a scattering event between two fermionic particles will also in general depend on the quantum state of the carrier gauge field. As an example, the electromagnetic field can be found in a so-called coherent state, which follows the classical Maxwell equations, or instead in a non-classical Fock state (also called photon number state), which contains a non-fluctuating fixed number of photons [1].

The following question can then be asked: How is the scattering between the constituents of matter affected by preparing the force carriers in different quantum states? See Fig. 1. This work revolves around this issue, which is so far largely unexplored. One reason for this lies in the fact that, in the context of high energy physics, a systematic experimental investigation is not feasible, as in particle colliders the gauge fields cannot be prepared in a desired quantum state.

On the other hand, the above question becomes relevant in a specific non-relativistic version of QED implemented within materials [2–4]. Here, by confining the light around matter (for instance using mirrors forming a resonator), a selected

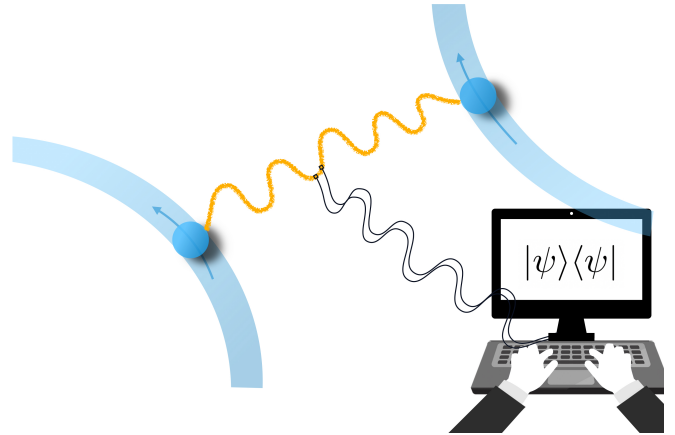


FIG. 1. Graphical representation of the basic idea: The scattering between the constituents of matter (blue spheres) is mediated by a force carrier (wiggled line), which is prepared in a given quantum state.

number of modes can be separated from the electromagnetic continuum, and standard techniques of quantum optics become available for the preparation of desired quantum states of photons. Importantly, mode confinement enhances the coupling between photons and electrons, so that the material is affected already by low-intensity electromagnetic fields, which are more easily prepared in non-classical states. Recent experimental developments now allow to prepare non-Gaussian states of structured light [5–8], where the dimensionality (both in real and frequency space) of entanglement is enlarged by multiple modes beyond the binary polarization space. Finally, the fact that this regime of QED is realized within a material at finite electron densities, allows to explore the effect of different quantum states of photons not only on individual scattering events between electrons, but also on emergent collective phenomena.

The possibility for experimental investigation also exists at

* ahana@physics.rutgers.edu

† piazza@pks.mpg.de

a less fundamental level, where the role of photons can be played by collective degrees of freedom like phonons [9, 10], or by excitons-(polaritons) [11, 12]. Also ultracold atomic mixtures [13, 14] offer a high degree of selective control which could allow for the preparation of certain quantum states of one of the components.

In order to answer our question of interest, an approach outside the scope of equilibrium scattering and many-body theory is needed, since the force-carrier part of the system is externally prepared in an arbitrary initial state. We achieve this by developing a tailored real-time formulation of the Dyson equation for the two-particle vertex function, known in thermal equilibrium as the Bethe-Salpeter equation [15]. The advantage of our approach is to reveal the difference between initial quantum states of the force carrier through an emergent structure of scattering vertices. This structure, which is irrelevant when the carrier is prepared in a Gaussian state, adds to the usual energy-momentum and causal structure of the scattering, and is determined by the wave function in the Hilbert-space of the force carrier. Moreover, our method is amenable to non-perturbative resummation techniques, allowing to describe collective phenomena, like instabilities towards macroscopically ordered phases.

The scenario under consideration also constitutes an interesting problem in the context of many-body dynamics, and specifically in regards to the issue of quantum thermalization [16–18]. If our interacting system of material particles and force carriers would be ergodic, the memory of the initial state of the carrier would be gradually lost with time, so that its influence on scattering and collective phenomena would be a transient effect. However, this is not necessary the case, for instance due to the fact that gauge theories are characterized by constraints which are able to prevent thermalization [19, 20]. The investigation of the role played by this type of so-called many-body localization phenomena in preserving some memory of the initial state of the force carrier constitutes a very intriguing line of research. In this first work however, we instead consider a different and less subtle mechanism for the preservation of the memory of the initial state, which is the absence of back action of the matter onto the force carrier. We show that this can be realized whenever there is a clear separation between the characteristic length and time scales of the matter and the force carriers [2, 21, 22]. These conditions are naturally met in QED within materials, where the electromagnetic-mode confinement can create a large energy gap for the photons, the latter being at the same time very delocalized over the material. These conditions allow to suppress the backaction of the electrons onto the photons to the extent that it becomes irrelevant over the timescales of interest, leaving us with a non-equilibrium, but time-independent problem, where the force carriers remain in the quantum state they were prepared in.

After developing the general framework, we concentrate on a specific example in the context of QED within materials: The case of photon mediated electron pairing and superconductivity. This recently proposed possibility provides a new scenario, with implementations both in two-dimensional materials [23, 24] and ultracold atomic gases [25–27]. In

particular, by considering a specific tight-binding model of QED, recent studies have found that, as an alternative to tuning the electromagnetic-mode energy, one can project the photon onto number states to control the sign of the effective light-mediated, static interaction potential [28], and thus favour pairing and superconductivity over competing instabilities [29]. A modification of the effective light-matter coupling constant could also be achieved by squeezing the photon field to enhance the proper quadrature entering the electromagnetic vector field, as proposed in the phonon case [30]. On the other hand, in a previous work [22] we have shown that, due to the above mentioned separation of scales characterizing QED within materials, pairing can actually be dominated by scattering processes which are not mediated by a static interaction vertex as in the usual Bardeen-Cooper-Schrieffer (BCS) scenario, but rather by resonant (non-adiabatic) photons. Here we demonstrate that exactly those non-BCS processes directly depend on the quantum state of the photon, and give thus rise to the emergent structure of scattering vertices for non-Gaussian states. In particular, by preparing the photons in pure Fock states, one can enhance pair correlations in a controlled way, thereby tuning the criticality and universality class of the superconducting phase transition by the choice of the number of photons. Our results also reveal that the thermal mixture of Fock states regularizes the strong pair fluctuations present in each of its components, yielding the usual BCS criticality.

II. SUMMARY OF THE MAIN RESULTS

1. For a generic form of the coupling between the fermionic matter and the bosonic mediator, using a real-time formulation on the Keldysh contour we derive the equation for the two-particle scattering vertex between two Fermions with the bosonic mediator initially prepared in an arbitrary quantum state. This equation, which we name Carrier-Hilbert-Space Bethe-Salpeter (CHSBS) equation, is shown schematically in Fig.2 for the particular case of a mediator initially prepared in a pure Fock state. In the CHSBS equation, the scattering vertex acquires, in addition to the usual frequency, momentum and causal (Keldysh) components, further components labelled by Fock indices, i.e., representing the Hilbert space of the force carrier. The couplings between the Hilbert-space components of the vertex are set by the initial quantum state of the force carrier. When the latter is Gaussian, these couplings are such that the emergent Hilbert-space structure in the CHSBS equation can be rearranged to become irrelevant, yielding the standard Bethe-Salpeter equation (see Fig.5). In the particular case of a mediator prepared in a pure Fock state, the emergent scattering structure involves coupling between vertices corresponding to different Fock states with a number of photons smaller than the initial one. It can be solved in a hierarchical fashion starting from the vacuum state.

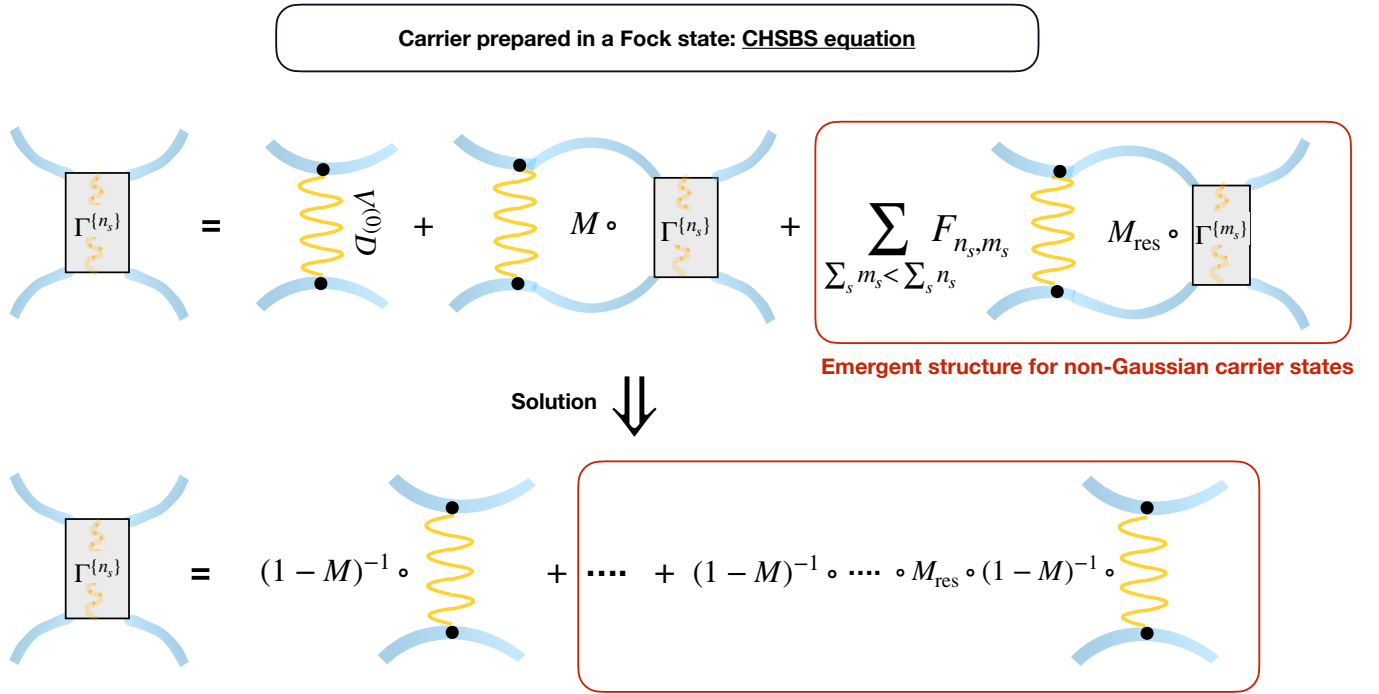


FIG. 2. Emergent scattering structure in the Carrier-Hilbert-Space Bethe-Salpeter (CHSBS) equation (see Eq.(32)). Schematic representation of the equation for the scattering vertex function $\Gamma^{\{n_s\}}$ between two Fermions (blue lines) mediated by a carrier Boson (wiggled line) initially prepared in a pure Fock state defined by the occupations $\{n_s\}$ of available modes labelled by s . The properties of the Boson are encoded in the Green's function D , while the form factor of the Boson-Fermion coupling is $V^{(0)}$. Two Fermionic blue lines meet with the Bosonic wiggled line at the Yukawa vertex (given in Eq.24) represented by black dots. The matrices M and M_{res} encode the momentum, frequency, and causal structure of the scattering (with the symbol \circ indicating the tensor product in all the corresponding spaces). In particular, M_{res} corresponds to scattering processes where a real mediator is fully absorbed/emitted by the Fermions. These processes are the ones depending on the quantum state of the mediator, and give rise to the emergent structure reflecting the Hilbert space of the latter. The vertex $\Gamma^{\{n_s\}}$ thus becomes coupled to vertices corresponding to different Fock-space occupations $\Gamma^{\{m_s\}}$, with the coupling function F_{n_s, m_s} . The bottom row represents the form of the iterative solution of the CHSBS equation (see Eq.(45)).

2. We apply the CHSBS equation to the computation of the pair-scattering vertex, for a specific QED setup where cavity photons mediate interactions between electrons at finite density. We compare the case where the photons are initially prepared in a Gaussian thermal state (where the emergent scattering structure is absent, see Fig.5) with the case in which they are prepared in a pure Fock state (inducing an emergent scattering structure of the type shown in Fig.2). We compute the critical properties of the superconducting phase transition. The results are summarized in Fig.3. The critical temperature for the case of photons prepared in a pure Fock state does not depend on the number of photons and equals the vacuum i.e. zero-photons critical temperature. The electron-electron vertex function in the pairing channel Γ_{pairing} diverges at the critical temperature with an exponent γ , which equals one in the standard BCS scenario where Bosons mediate simply a static attractive interaction. For photons prepared in a Fock state, we find instead that γ grows linearly with n_0 , and the electron pair correlation length ξ as $\sqrt{1 + n_0}$. The increased critical pair fluctuations present when the photon is prepared in number states are regularized in

the thermal mixture, where the γ and ξ are independent of the photon number and agree with the BCS prediction, while the critical temperature is increased with respect to the vacuum case by a factor dependent on the photon number. Finally, the exponent ν describing the divergence of the correlation length at the critical point remains the same in both cases, and corresponds to the BCS prediction.

III. STRUCTURE OF THE MANUSCRIPT

In Section IV we provide a brief review of the background formalism. In Section V we derive our CHSBS equation. From Section VI on, we specify to the cavity QED model where photons mediate pairing between electrons, and compute the critical properties of the superconducting transition in Section VII. In Section VIII, we discussed justification of the time-independent approach we used to study the case of cavity-mediated superconductivity. Finally, in Section IX we provide concluding remarks and a brief outlook.

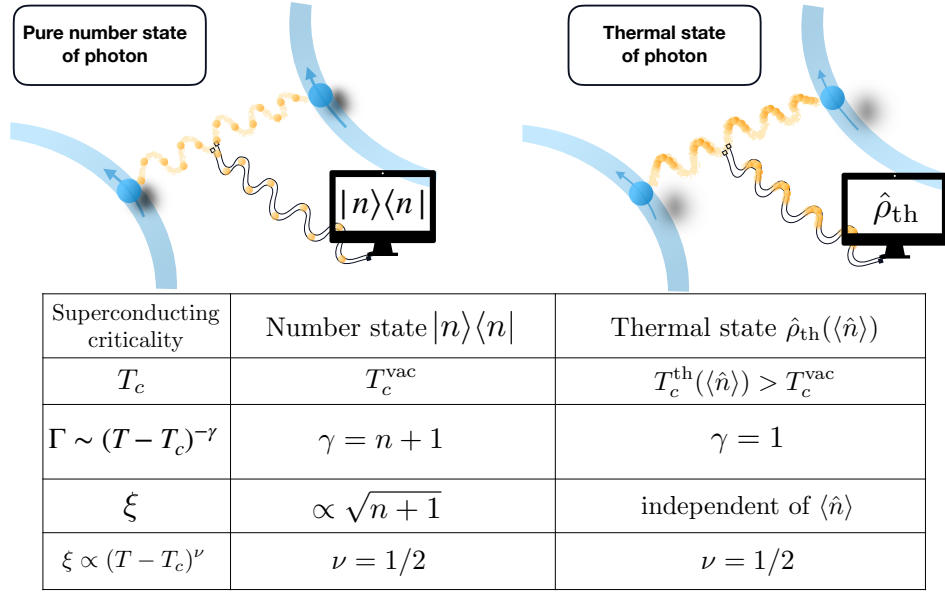


FIG. 3. Controlling the superconducting critical behavior of electrons by preparing the quantum state of the mediator photon in cavity QED. The CHSBS equation (see Fig.2) is solved in the pairing channel at the superconducting critical point. Two quantum states of the carrier photons are compared: a pure Fock state with n Bosons, and a thermal mixture (Eq. (6) with average number of photons $\langle\hat{n}\rangle$). Different critical properties are considered: the critical temperature T_c (see Section VII A), the susceptibility exponent (see Section VII B), the correlation length ξ and its critical exponent ν (see Section VII C).

IV. BACKGROUND FORMALISM

The approach employed in this work is based on the Schwinger-Keldysh field theory (KFT), which is an action-based formalism able to describe quantum many-body systems out of equilibrium. The Keldysh partition function, Z is defined from the time-evolving density matrix $\hat{\rho}(t)$ as $Z = \text{Tr}[U(\infty, 0)\hat{\rho}(0)U(0, \infty)]$, where $U(t, 0)$ and $U(0, t)$ are the forward and backward time evolution operators, respectively. These are represented by two path integrals, each involving one of two independent fields, $\chi_+(t)$ and $\chi_-(t)$ [31]. These two pieces of the path-integral contour are connected at $t = 0$ by the matrix element, $\langle\chi_+(0)|\hat{\rho}(0)|\chi_-(0)\rangle$ of the density matrix of the system at the initial time, as

$$Z = \int D[\chi_+, \chi_-] e^{i[S_{\text{ev}}(\chi_+) - S_{\text{ev}}(\chi_-)]} \langle\chi_+(0)|\hat{\rho}(0)|\chi_-(0)\rangle. \quad (1)$$

Here, S_{ev} is the action describing the time-evolution of the system over the forward and the backward contour.

We start by considering a system of non-interacting bosonic/fermionic particles, described by the Hamiltonian

$$H_0 = \sum_s \omega_s b_s^\dagger b_s. \quad (2)$$

Here b_s^\dagger is the creation operator of the Bosons/Fermions in the single-particle state labeled by the index s , satisfying the usual commutation/anticommutation relations $(b_s b_s^\dagger \mp b_s^\dagger b_s) = 1$, with the convention where the upper/lower sign applies to the Bosons/Fermions. In this non-interacting case the action is

simply

$$S_{\text{ev}}(\chi_\pm) = \int_{-\infty}^{\infty} dt \sum_s \chi_\pm^*(s, t) (i\partial_t - \omega_s) \chi_\pm(s, t). \quad (3)$$

We will be interested in computing the Green's functions (GFs) of the system. For this purpose we define the generating functional, which is obtained from Z by adding sources $J_\pm(t)$ which couple linearly to the fields χ_+ and χ_- as [31],

$$Z[J] = \int D[\chi_+, \chi_-] e^{i[S_{\text{ev}}(\chi_+) - S_{\text{ev}}(\chi_-)]} \langle\chi_+(0)|\hat{\rho}(0)|\chi_-(0)\rangle \times e^{i(\int_s dt J_+^*(s, t)\chi_+(s, t) - \int_s dt J_-^*(s, t)\chi_-(s, t) + h.c.)}. \quad (4)$$

Due to the constraint imposed by the conservation of probability and causality, not all GFs are independent. It is thus useful to work in the rotated basis of classical $\chi_{cl} = (\chi_+ + \chi_-)/\sqrt{2}$ and quantum fields $\chi_Q = (\chi_+ - \chi_-)/\sqrt{2}$. For instance, among the one-particle GFs, only two out of four are independent, namely the retarded and the Keldysh (also called statistical) GF. Those are defined as,

$$G_R(s, t, t') = -i\langle\chi_{cl}(s, t)\chi_Q^*(s', t')\rangle = \frac{i\partial^2 Z[J]}{\partial J_Q^*(s, t)\partial J_{cl}(s', t')}$$

$$G_K(s, t, t') = -i\langle\chi_{cl}(s, t)\chi_{cl}^*(s', t')\rangle = \frac{i\partial^2 Z[J]}{\partial J_Q^*(s, t)\partial J_Q(s', t')}, \quad (5)$$

where $J_{cl, Q} = (J_+ \pm J_-)/\sqrt{2}$ are the classical and quantum component of the linear sources. As the nomenclature suggests, G_R represents the retarded evolution of the system

governed by the dispersion (and the lifetime) of the modes, and hence does not depend on the initial conditions. On the other hand, G_K explicitly depends on the initial conditions carrying their memory during the time-evolution.

In order to proceed and derive equations of motions for the GFs, we have to deal with the matrix element of the initial state. As illustrated in the next two Sections, we will do this by exponentiating the matrix element of the initial state, so that Z can be expressed as a path-integral with an action which incorporates both the information about the initial conditions as well as the time-evolution under the Hamiltonian dynamics.

A. Single-particle Green's functions for thermal initial states

In this sub-Section, we will illustrate how to incorporate the matrix element of the initial state in the action for a thermal initial condition and obtain the GFs. We consider a Gaussian thermal initial density matrix at temperature $T = 1/\beta$ given by,

$$\hat{\rho}(0) = \hat{\rho}_{\text{th}} = \frac{\sum_{\{n_s\}} e^{-\beta \sum_s \omega_s n_s} |\{n_s\}\rangle \langle \{n_s\}|}{\sum_{\{n_s\}} e^{-\beta \sum_s \omega_s n_s}}, \quad (6)$$

with $|\{n_s\}\rangle = |n_1, n_2, \dots\rangle$ being a Fock state with n_1 particles in the mode 1, n_2 in the mode 2, etc.. In this case, the matrix element of the initial state can be readily exponentiated as a bilinear term of the initial fields as [31],

$$\langle \chi_+(0) | \hat{\rho}(0) | \chi_-(0) \rangle = e^{\pm \sum_s \rho_s \chi_+^*(s,0) \chi_-(s,0)}, \quad (7)$$

where $\rho_s = \exp(-\beta \omega_s)$. Hence, the information about the thermal initial conditions can be easily added as a quadratic (bi-linear) term in the action as

$$Z = \int D[\chi_+, \chi_-] e^{i[S_{\text{ev}}(\chi_+) - S_{\text{ev}}(\chi_-) + \delta S(\chi_+^*, \chi_-; \rho_s)]},$$

with

$$\delta S(\chi_+^*, \chi_-; \rho_s) = \mp i \sum_s \rho_s \chi_+^*(s,0) \chi_-(s,0). \quad (8)$$

This makes systems starting from Gaussian thermal initial density matrices amenable to the standard KFT techniques [31]. For non-interacting systems (evolving with the Hamiltonian given in Eq. (2)), the whole action is quadratic and the functional integrals over the fields can be performed exactly to yield the one-particle GFs,

$$\begin{aligned} G_R(s, t, t') &= -i \Theta(t - t') e^{-i\omega_s(t-t')}, \\ G_K(s, t, t') &= -i \frac{1 \pm \rho_s}{1 \mp \rho_s} e^{-i\omega_s(t-t')}, \end{aligned} \quad (9)$$

where $(1 \pm \rho_s)/(1 \mp \rho_s) = 1 \pm 2n_{B(F)}$ is related to the Bose/Fermi distribution $n_{B(F)}$ in thermal equilibrium.

B. Single-particle Green's functions with arbitrary initial states

For an arbitrary $\hat{\rho}(0)$, exponentiation of its matrix element in Eq. (1) can not be performed to obtain a δS containing only bi-linear terms involving the initial fields $\chi_+(0)$ and $\chi_-(0)$. Hence, even non-interacting systems starting from non-thermal states $\hat{\rho}(0)$ yield a non-Gaussian field theory which cannot be treated exactly within the standard KFT. Recently, in Ref. 32, an efficient prescription has been proposed to exponentiate $\hat{\rho}(0)$ within the action-based KFT formalism, which we will briefly review here.

To illustrate this, we first assume that the system is initialized in a pure Fock state $|\{n_s\}\rangle = |n_1, n_2, \dots\rangle$,

$$\hat{\rho}(0) = |\{n_s\}\rangle \langle \{n_s\}|. \quad (10)$$

In this case, $\langle \chi_+(0) | \hat{\rho}(0) | \chi_-(0) \rangle$ can be exponentiated by introducing a quadratic source u_s which couples to the bi-linears of the initial fields $\chi_+^*(s,0) \chi_-(s,0)$ for all the modes s , and finally taking appropriate derivatives w.r.t u_s . For the state given in Eq.(10), the matrix element can be written as

$$\langle \chi_+(0) | \hat{\rho}(0) | \chi_-(0) \rangle = \mathcal{L} e^{\pm \sum_s u_s \chi_+^*(s,0) \chi_-(s,0)} \Bigg|_{u_s=0}, \quad (11)$$

where the derivative operator,

$$\mathcal{L} = \prod_s \frac{1}{n_s!} \left(\frac{\partial}{\partial u_s} \right)^{n_s} \quad (12)$$

encodes the information about the initial Fock state.

The corresponding partition function of the system can be thus written as

$$Z = \mathcal{L} \left[\int D[\chi_+, \chi_-] e^{i[S_{\text{ev}}(\chi_+) - S_{\text{ev}}(\chi_-) + \delta S(\chi_+^*, \chi_-; u)]} \right] \Bigg|_{u_s=0},$$

with

$$\delta S(\chi_+^*, \chi_-; u) = \mp i \sum_s u_s \chi_+^*(s,0) \chi_-(s,0). \quad (13)$$

The prescription for computing the GFs is then organized in two steps.

(i) Define an intermediate u_s -dependent partition function in presence of the linear, J_{\pm} , and quadratic, u_s sources,

$$\begin{aligned} Z[J; u] &= \int D[\chi_+, \chi_-] e^{i[S_{\text{ev}}(\chi_+) - S_{\text{ev}}(\chi_-) + \delta S(\chi_+^*, \chi_-; u)]} \times \\ & e^{i(\int \sum_s dt J_+^*(s,t) \chi_+(s,t) - \int \sum_q dt J_-(s,t) \chi_-(s,t) + h.c)} \end{aligned} \quad (14)$$

By taking derivatives of $Z[J; u]$ w.r.t. the linear sources we obtain an intermediate $\{u_s\}$ -dependent Green's functions $G(s, t, t'; u)$ as,

$$\frac{i \partial^2 Z[J; u]}{\partial J^*(s, t) \partial J(s, t')} = \left[\prod_s (1 \mp u_s)^{\mp 1} \right] G(s, t, t'; u), \quad (15)$$

where we omitted the contour indices for simplicity. At this point it is important to note that the normalization of the intermediate partition function $Z[J = 0; u] = \prod_s (1 \mp u_s)^{\mp 1}$ crucially depends on the initial sources $\{u_s\}$ and hence we need to keep it explicitly in the path integral (unlike the Gaussian thermal case where $Z[J = 0] = (1 \mp \rho_s)^{\mp 1} = 1$). The intermediate retarded and Keldysh Green's functions take the form,

$$\begin{aligned} G_R(s, t, t'; u) &= -\mathbf{i}\Theta(t - t')e^{-\mathbf{i}\omega_s(t-t')} \\ G_K(s, t, t'; u) &= -\mathbf{i}\frac{1 \pm u_s}{1 \mp u_s}e^{-\mathbf{i}\omega_s(t-t')}, \end{aligned} \quad (16)$$

where the retarded component is (as expected) independent of the initial sources and hence the information about the initial conditions of the system is solely carried by the Keldysh component.

(ii) Take the derivatives of $G(s, t, t'; u)$ w.r.t. $\{u_s\}$ to calculate the physical GFs $G(s, t, t')$ of the system. This yields

$$\begin{aligned} G_R(s, t, t') &= \mathcal{L} \left[\prod_s (1 \mp u_s)^{\mp 1} G_R(s, t, t'; u) \right] \Bigg|_{u_s=0} \\ &= -\mathbf{i}\Theta(t - t')e^{-\mathbf{i}\omega_s(t-t')} \\ G_K(s, t, t') &= \mathcal{L} \left[\prod_s (1 \mp u_s)^{\mp 1} G_K(s, t, t'; u) \right] \Bigg|_{u_s=0} \\ &= -\mathbf{i}(1 \pm 2n_s)e^{-\mathbf{i}\omega_s(t-t')}. \end{aligned} \quad (17)$$

Here, for the sake of simplicity of the notation, we use G with an explicit u dependence in the argument as an intermediate GF, while the one without such dependence is the physical GF.

We note that interchanging the order of taking derivatives w.r.t. J and u is permissible, as J are linear sources and u quadratic sources. This is crucial for the major simplifications allowed by this method [32] (see also next Section).

An immediate extension of the above formalism for initial pure Fock states is to include a density matrix which is diagonal in the Fock basis,

$$\hat{\rho}(0) = \sum_{\{n_s\}} c_{\{n_s\}} |\{n_s\}\rangle \langle \{n_s\}|, \quad (18)$$

where $\sum_{\{n_s\}} c_{\{n_s\}} = 1$. In this case the derivative operator which encodes the information about $\hat{\rho}(0)$ takes the form

$$\mathcal{L} = \sum_{\{n_s\}} c_{\{n_s\}} \prod_s \frac{1}{n_s!} \left(\frac{\partial}{\partial u_s} \right)^{n_s}. \quad (19)$$

As before, applying \mathcal{L} on the intermediate $\{u_s\}$ -dependent Green's functions $G(s, t, t'; u)$ (together with the $\{u_s\}$ -dependent normalization) we obtain the final physical Keldysh GF,

$$G_K(s, t, t') = -\mathbf{i} \sum_{\{n_s\}} c_{\{n_s\}} (1 + 2n_s) e^{-\mathbf{i}\omega_s(t-t')}, \quad (20)$$

while the retarded component of the correlation function remains unaffected by the initial condition and is given by Eq. (17).

We note that in both the examples of initial density matrices given above in Eq. (10) and (18), the dynamics of the system is invariant under time-translation as the Hamiltonian is diagonal in the same Fock basis. The time-translation invariance is broken when we consider a generic initial density matrix of the multi-mode system which also has non-diagonal elements expanded in the Fock basis. Within this extended KFT formalism, we can deal with a generic number-conserving $\hat{\rho}(0)$ of the form,

$$\hat{\rho}(0) = \sum_{\{n_s\}, \{m_s\}} c_{\{n_s\}, \{m_s\}} |\{m_s\}\rangle \langle \{n_s\}|, \quad (21)$$

with the constraint $\sum_s n_s = \sum_s m_s$. In this case the physical Keldysh GF becomes a function of two time variables:

$$G_K(s, s', t, t') = -\mathbf{i} (1 + 2\langle b_s^\dagger b_{s'} \rangle_0) e^{-\mathbf{i}(\omega_s t - \omega_{s'} t')}, \quad (22)$$

while the retarded GF is unaffected by the initial condition and thus remains time-translation invariant. In this case, the system exhibits a non-trivial time-evolution induced by the memory of the initial state.

V. VERTEX FUNCTION FOR FORCE CARRIERS INITIALIZED IN ARBITRARY QUANTUM STATES

After having reviewed how to compute single-particle GF in a system of Bosons or Fermions initialized in a non-Gaussian, non-thermal state, we now turn to the case of interest, which is the one where Fermions (the constituents of matter) interact with Bosons (the force carriers) via a Yukawa type coupling, and the Bosons are initialized in a non-thermal state. We will be interested in studying how Fermion-Fermion scattering mediated by the Boson, and ultimately collective phenomena, are affected by the state in which the Boson is initialized. This requires us to develop an extension of the standard Dyson equation for the two-particle vertex function (also called Bethe Salpeter equation), allowing to deal with the memory of the non-thermal, non-Gaussian initial conditions of the Boson.

The fermionic matter is initialized in a thermal density matrix given Eq. (6). The contribution to the non-interacting part of the action coming from the Fermions is $S_F(\psi_{cl}, \psi_Q)$ defined in terms of the Grassmann fields ψ_{cl}, ψ_Q . This takes the thermal form composed of Eqs. (3) and (8). By inverting S_F we can obtain the non-interacting fermionic GFs given in Eqs. (9). On the other hand, the Bosons are initialized to the generic diagonal density matrix given in Eq. (18), which covers a broad class of initial conditions. Differently from the fermionic counterpart, the non-interacting bosonic action has the contribution given by Eq. (13), which depends on the initial quadratic source u . It is useful to express the bosonic action $S_B(X_{cl}, X_Q; u)$ in terms of real position (also called quadrature) fields $X_{cl, Q}$, yielding the non-interacting u -dependent

(intermediate) bosonic GFs of the form,

$$\begin{aligned} D_K(s, t, t'; u) &= -\mathbf{i} \frac{1 + u_s \cos(\omega_s(t - t'))}{1 - u_s} \frac{1}{2\omega_s}, \\ D_R(s, t, t') &= -\Theta(t - t') \frac{\sin(\omega_s(t - t'))}{2\omega_s}. \end{aligned} \quad (23)$$

We consider the following form of the Yukawa-type coupling

$$H_{\text{int}} = \sum_{k, k', s} \sqrt{2\omega_s} g_{k, k', s} c_{k'}^\dagger c_k X_s, \quad (24)$$

where c^\dagger is the creation operator of the Fermions and X the position operator of the Bosons. The corresponding part of the action reads

$$\begin{aligned} S_{\text{int}} &= - \int_{-\infty}^{\infty} dt \sum_{k, k', s} g_{k, k', s} \sqrt{2\omega_s} \times \\ &\left[\{\psi_{cl}^*(k', t) \psi_Q(k, t) + cl \leftrightarrow Q\} X_{cl}(s, t) \right. \\ &\left. + \{\psi_{cl}^*(k', t) \psi_{cl}(k, t) + cl \leftrightarrow Q\} X_Q(s, t) \right]. \end{aligned} \quad (25)$$

After integrating out the bosonic degrees of freedom (which can be done exactly), we obtain the intermediate partition function $Z[u]$ involving only fermionic fields of the form,

$$Z[u] = \frac{1}{\prod_s (1 - u_s)} \int D[\psi_{cl, Q}] e^{\mathbf{i} S_F(\psi_{cl}, \psi_Q) + \mathbf{i} S_{\text{eff}}(\psi_{cl}, \psi_Q; u)}, \quad (26)$$

where the four-Fermion interaction term mediated by the Bosons has the following structure,

$$S_{\text{eff}}(\psi_{cl}, \psi_Q; u) = - \int dt dt' \sum_{\{k_i\}, s} V^{(0)}(\{k_i\}, s) D(s, t, t'; u) \times \psi^*(k_1, t) \psi^*(k_2, t') \psi(k_3, t') \psi(k_4, t). \quad (27)$$

The strength of the quartic interaction is $V^{(0)}(\{k_i\}, s) = \omega_s g_{k_3, k_4, s} g_{k_1, k_2, s}^*$. Here we have omitted all Keldysh indices for the sake of simplicity, since the results of the present section can be illustrated without explicit reference to the Keldysh structure. This does not mean the latter is not important, as the memory of the initial quantum state in which the carrier Boson is prepared is encoded only in the Keldysh component of $D(s, t, t'; u)$. Due to the causality structure of the theory, each component of $D(s, t, t'; u)$ can appear only together with certain combinations of the (cl, Q) indices of the Fermion fields. We refer to Appendix A for a detailed discussion.

The physical partition function of the system is obtained by taking the appropriate set of derivatives of $Z[u]$ w.r.t. $\{u_s\}$ through the operator \mathcal{L} . The detailed form of the operator \mathcal{L}

depends the specific form of $\hat{\rho}(0)$ of the Bosons. For the particular case considered in this Section in Eq. (18), \mathcal{L} is given by Eq. (19). As illustrated in the previous Section, to calculate the physical GFs of the interacting Fermions, we add linear sources $J(k, t)$ coupled to the fields $\psi(k, t)$ at all times t , and then take derivatives of the physical generating functional $Z[J]$ w.r.t. J to obtain the m -particle physical GF $G_m^F(k_1, \dots, k_m, t_1, \dots, t_m)$.

The non-linearity of the derivative operator \mathcal{L} , together with the presence of the crucial u_s -dependent normalization $1/\prod_s(1 - u_s)$ of the partition function, makes several useful properties of the theory, which could be exploited for Gaussian thermal initial conditions, inapplicable here. A major complication comes from the fact that Wick's theorem cannot be used to factorize the physical higher-order GFs in terms of two-point GFs when the action is Gaussian [32]. This leads to the breakdown of standard perturbative and non-perturbative approximations, like the Dyson or Bethe-Salpeter equations normally used for systems initialized in a Gaussian thermal state [15]. In order to overcome these problems in our specific computation of the Fermion-Fermion vertex function with a force carrier prepared in a non Gaussian initial state, we adopt a two-step procedure like the one used for the case of purely bosonic/fermionic model of Section IV B. After having integrated out the force carrier, we are dealing with a purely fermionic action. We first define an intermediate $\{u_s\}$ -dependent GF $G_m^F(k_1, \dots, k_{2m}, t_1, \dots, t_{2m}; u)$ obtained from $Z[J, u]$ by taking derivatives with respect to the J 's, and subsequently take the final derivatives w.r.t $\{u_s\}$ via the operator \mathcal{L} to obtain the physical GF $G_m^F(k_1, \dots, k_{2m}, t_1, \dots, t_{2m})$. Even though we employ the same procedure, the structure of the resulting equations in our case is very different from the one obtained for a purely fermionic theory where the interactions are not mediated by a force carrier and the Fermions themselves are initialized in a non-Gaussian state. The reason is that in our case the operator \mathcal{L} acts on the interaction part of the action S_{eff} as it contains the carrier GF, while in the purely fermionic case \mathcal{L} acts only on the quadratic part δS . Although taking derivatives w.r.t $\{u_s\}$ and obtaining a closed expression for G_m^F can be non-trivial, the above two-step construction makes the problem manageable in the best possible way: at the intermediate stage we can exploit all the useful properties also available in the Gaussian thermal case for approximating the equations for the GFs, and in particular diagrammatic perturbative approaches and resummation techniques to obtain the intermediate $G_m^F(u)$.

The next step is now to derive the equation for the vertex function. We will focus on two-particle vertices, and start from the two-particle physical GF, $G_2^F(k_1, \dots, k_4, t_1, \dots, t_4) = \mathcal{L}[G_2^F(k_1, \dots, k_4, t_1, \dots, t_4; u) / \prod_s(1 - u_s)]|_{u_s=0}$. The intermediate $G_2^F(k_1, \dots, k_4, t_1, \dots, t_4; u)$ can be formally constructed as a perturbation expansion in terms of the intermediate two particle vertex function $\Gamma(k_1, \dots, k_4, t_1, \dots, t_4; u)$ defined as,

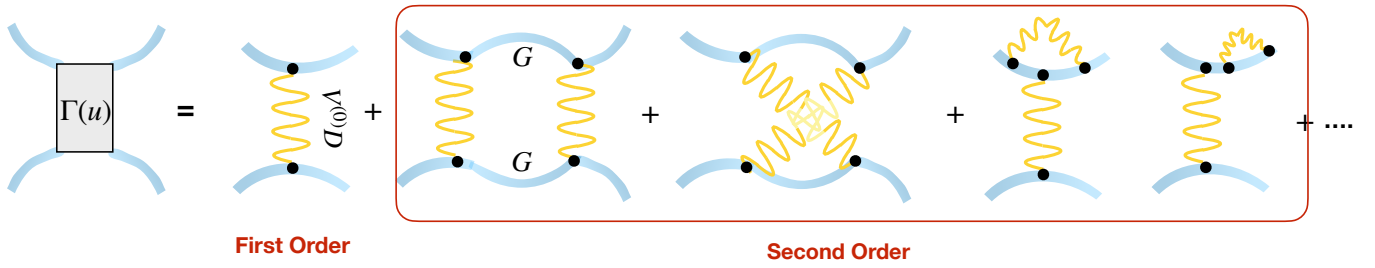


FIG. 4. The perturbative expansion of the intermediate vertex function $\Gamma(u)$, which takes the same form as in the thermal-equilibrium case [15]. The diagrams are arranged in powers of the coupling factor $V^{(0)}(\{k_i\}, s)$, and are shown up to second order. Fermions are represented by solid blue lines (G is the non-interacting Fermionic Green's function) while the carrier Bosons are represented by yellow wiggled lines. At first order, $\Gamma(u)$ is simply the bare interaction vertex $\Gamma(u) = V^{(0)}(\{k_i\}, s)D(s, t, t'; u)$. Similarly, in all higher order diagrams, the u_s dependence is solely coming through the carrier GF $D(s, t, t'; u)$, and the contribution from the carrier initial state in each diagram can be computed analytically.

$$G_2^F(k_1, \dots, k_4, t_1, \dots, t_4; u) = \int \prod_i dt_i G(k_1, t_1, t'_1) G(k_2, t_2, t'_2) G(k_3, t_3, t'_3) G(k_4, t_4, t'_4) \Gamma(k_1, \dots, k_4, t'_1, \dots, t'_4; u). \quad (28)$$

Here the external points at times t_i are connected to the internal points at time t'_i by non-interacting Fermion GFs G (independent of $\{u_s\}$), and the effects of the Fermion-Fermion interactions are included in the definition of Γ , which thus solely carries the $\{u_s\}$ dependence [33]. The physical two-particle vertex function is then given by,

$$\Gamma(k_1, \dots, k_4, t_1, \dots, t_4) = \mathcal{L} \left[\frac{\Gamma(k_1, \dots, k_4, t_1, \dots, t_4; u)}{\prod_s (1 - u_s)} \right] \Bigg|_{u_s=0}. \quad (29)$$

This function contains all the information about the initial state of the force carrier, and thus gives a self-contained quantity to investigate how the latter affects the Fermion-Fermion scattering. Moreover, a divergence in the physical vertex function signals an instability towards a macroscopically ordered phase where the corresponding fermionic bilinear acquires a finite expectation value. We will consider the example of pairing and superconductivity in Section VI.

Now we turn our attention to the construction a diagrammatic expansion of the intermediate vertex function $\Gamma(u)$. The simplest one is a perturbative expansion in powers of the quartic interaction potential $V^{(0)}(\{k_i\}, s)$ as shown in Fig. 4. Each Boson line corresponds to $D(s, t, t'; u)$ and carries the $\{u_s\}$ dependence coming from the initial state. Hence, if we truncate the perturbation series at certain order (say n , see Fig. 4), the u_s dependence of the a given diagram has an analytic form $(1 + u_s)^p / (1 - u_s)^{p+1}$ (including the normalization) with $p \leq n$, where the equality holds for the diagram where each carrier GF is a Keldysh GF. This means that the action of the derivative operator \mathcal{L} can be computed exactly to obtain a closed-form analytical answer for the physical vertex Γ .

A perturbative computation of Γ is however not sufficient to capture collective phenomena in many cases, the most prominent one being the description of instabilities towards macroscopically ordered phases. The required non-perturbative

closed-form equation can be derived for the intermediate vertex $\Gamma(u)$. We demonstrate this using a widely used resummation technique for a selected class of diagrams, called ladder resummation (corresponding to the leftmost of the second-order diagrams in Fig. 4), applied to $\Gamma(u)$:

$$\Gamma(u) = V^{(0)}D(u) + V^{(0)}D(u) \circ G \circ G \circ \Gamma(u) \quad (30)$$

where \circ stands for the appropriate integration or summation of the internal indices in position, time, and Keldysh space, and $V^{(0)}D(u)$ is the bare vertex function in the infinite series. The above equation can be rewritten as,

$$\Gamma(u) = V^{(0)}D(u) + M_{\text{nonres}} \circ \Gamma(u) + f(u)M_{\text{res}} \circ \Gamma(u). \quad (31)$$

Here, we have separated the u -independent contribution (2nd term in R.H.S.), containing $D_{R,A}$, from the u -dependent contribution, $f(u)$, containing $D_K(u)$. The rest (including $V^{(0)}, G$ and $D(u = 0)$) has been absorbed into the tensors M_{nonres} and M_{res} . The subscript M_{res} here refers to resonant processes involving the absorption/emission of a real (as opposed to virtual) force carrier. It is physically clear that it is those processes that depend on the quantum state of the carrier. Here the ladder is constructed out of the non-interacting fermionic GFs, G , which will simplify the computation of the physical vertex as the $\{u_s\}$ -derivatives will act only on the carrier GFs. This type of ladder resummation scheme is the standard approximation applied in thermal equilibrium to study instabilities associated with a divergence of Γ [15].

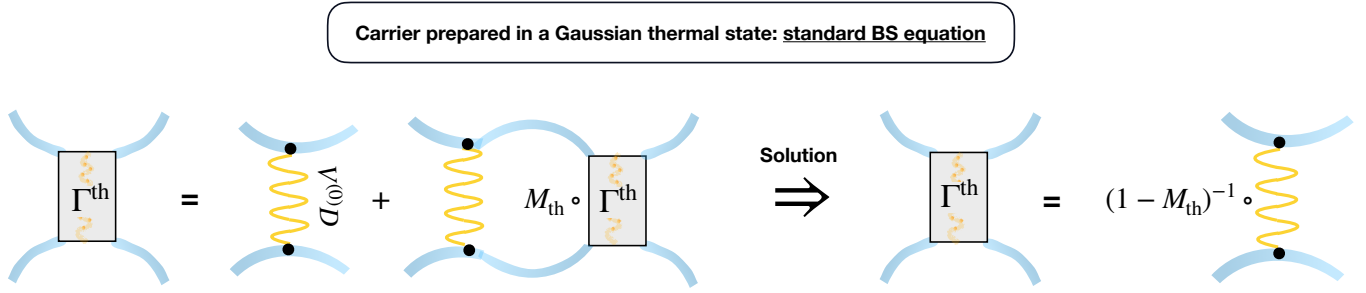


FIG. 5. Scattering structure in the standard Bethe-Salpeter (BS) equation (see Eq.(47)). Schematic representation of the equation for the scattering vertex function Γ^{th} between two Fermions (blue lines) mediated by a carrier Boson (wiggled line) initially prepared in a Gaussian thermal state. The properties of the Boson are encoded in the Green's function D , while the form factor of the Boson-Fermion coupling is $V^{(0)}$. The matrix M_{th} encodes the momentum, frequency, and causal structure of the scattering (with the symbol \circ indicating the tensor product in all these spaces). The scattering structure can be directly solved by inverting the corresponding matrix (see Eq.(38)).

A. Carrier initialized in a pure Fock state

Here we will compute the physical Γ for carriers initialized in a pure Fock state $\hat{\rho}(0) = |\{n_s\}\rangle\langle\{n_s\}|$. In this case the physical vertex $\Gamma^{\{n_s\}}$ is obtained by substituting Eq. (31) in Eq. (29) and then taking the derivatives with respect to the sources:

$$\Gamma^{\{n_s\}} = \prod_s \frac{1}{n_s!} \left(\frac{\partial}{\partial u_s} \right)^{n_s} \left[\frac{\Gamma(u)}{\prod_r (1 - u_r)} \right],$$

to obtain

$$\Gamma^{\{n_s\}} = V^{(0)}D + M \circ \Gamma^{\{n_s\}} + \sum_{\substack{\{p_s\} \\ \sum_s p_s < \sum_s n_s}} F_{n_s - p_s} M_{\text{res}} \circ \Gamma^{\{p_s\}}, \quad (32)$$

with

$$F_{n_s - p_s} = \frac{[(\partial/\partial u_s)^{n_s - p_s} f(u_s)]}{(n_s - p_s)!} \text{ and } M = M_{\text{nonres}} + M_{\text{res}}.$$

The physical vertex function for the generic initial density matrix shown in Eq. (18) can then be constructed as $\Gamma = \sum_{\{n_s\}} c_{\{n_s\}} \Gamma^{\{n_s\}}$.

Equation (32) is the main result here. This new tool provides the desired generalization of the Bethe-Salpeter equation for the vertex function to the situation where the force carrier is initialized in a Fock state (or an arbitrary mixture of Fock states). Equation (32), schematically represented in Fig2, clearly shows how this generalized form of the equation contains an additional structure with respect to the standard Bethe-Salpeter equation, since it involves a new set of vertices (or components of the vertex tensor), each corresponding to a different Fock state. These additional components satisfy a set of coupled equations of the Dyson type. Since each of the additional components of the vertex tensor corresponds to a given Fock state, one can think of this extra structure being a representation of the Hilbert space of the force carrier. This is why we named the above equation ‘‘Carrier-Hilbert-Space Bethe-Salpeter’’ (CHSBS) equation. For a force carrier initial-

ized in a given Fock-state, we see that the CHSBS equation involves a vertex component for that Fock state, plus an additional vertex component for each of all the Fock states with a smaller number of Bosons. The corresponding set of coupled Dyson equations can be inverted as

$$\Gamma^{\{n_s\}} = (1 - M)^{-1} \circ \left[V^{(0)}D + \sum_{\substack{\{p_s\} \\ \sum_s p_s < \sum_s n_s}} F_{n_s - p_s} M_{\text{res}} \circ \Gamma^{\{p_s\}} \right] \quad (33)$$

and then solved in an iterative manner starting from the vertex component corresponding to the Fock vacuum state ($n_s = 0 \forall s$),

$$\Gamma^{\{0\}} = (1 - M)^{-1} \circ [V^{(0)}D]. \quad (34)$$

B. Recovering the thermal-equilibrium Bethe-Salpeter equation

In this sub-Section, starting from the generally applicable (CHSBS) equation, we will recover the standard Bethe-Salpeter equation for the two-particle vertex function for the case where the carrier Bosons are in a Gaussian thermal state at equilibrium with the Fermions. This is by far not simply a sanity check for our CHSBS approach, but also physically very insightful. As will shall see next, it shows that the thermal density matrix given in Eq.(6) is a special mixture of all the Fock states which allows for a rearrangement of the emergent Hilbert-space structure in the CHSBS equation, such that this additional structure becomes irrelevant.

To illustrate this, we take the example of a fermionic system coupled to a single mode of Bosons where the physical two-particle vertex function Γ^{th} of the system in the thermal case can be constructed from the weighted average of the vertex

function of the constituent Fock states Γ^n as,

$$\Gamma^{\text{th}} = \frac{\sum_n e^{-\beta\omega n} \Gamma^n}{\sum_n e^{-\beta\omega n}}. \quad (35)$$

Substituting Γ^n from Eq.(32), we get,

$$\Gamma^{\text{th}} = V^{(0)} D + M \circ \Gamma^{\text{th}} + \frac{1}{\sum_n e^{-\beta\omega n}} \sum_n e^{-\beta\omega n} \sum_{p < n} F_{n-p} M_{\text{res}} \circ \Gamma^p. \quad (36)$$

The last term on the R.H.S., which is the additional structure characterizing the CHSBS equation, can be rearranged as,

$$\begin{aligned} & \frac{1}{\sum_p e^{-\beta\omega p}} \left[\left(\sum_{n=1}^{\infty} e^{-\beta\omega n} F_n \right) M_{\text{res}} \circ \Gamma^0 + \left(\sum_{n=2}^{\infty} e^{-\beta\omega n} F_{n-1} \right) M_{\text{res}} \circ \Gamma^1 + \left(\sum_{n=3}^{\infty} e^{-\beta\omega n} F_{n-2} \right) M_{\text{res}} \circ \Gamma^2 + \dots \right] \\ & = \left(\sum_{n=1}^{\infty} e^{-\beta\omega n} F_n \right) M_{\text{res}} \circ \sum_{p=0}^{\infty} \Gamma^p e^{-\beta\omega p} \frac{1}{\sum_p e^{-\beta\omega p}} = \left(\sum_{n=1}^{\infty} e^{-\beta\omega n} F_n \right) M_{\text{res}} \circ \Gamma^{\text{th}}. \end{aligned} \quad (37)$$

This means that the CHSBS equation for Γ^{th} given in Eq. (36) can be directly closed without having to solve the emergent Hilbert-space structure, yielding

$$\Gamma^{\text{th}} = V^{(0)} D + M_{\text{th}} \circ \Gamma^{\text{th}}, \quad (38)$$

where $M_{\text{th}} = M + \left(\sum_{n=1}^{\infty} e^{-\beta\omega n} F_n \right) M_{\text{res}}$.

The above line of arguments can be easily generalized to multi-mode Bosons to recover the structure of the standard BS equation in thermal equilibrium shown in Fig.5.

VI. SUPERCONDUCTIVITY MEDIATED BY CAVITY PHOTONS PREPARED IN NON-GAUSSIAN STATES

In the previous Section, we have considered a generic system of Fermions interacting with a bosonic field via a Yukawa-type coupling. We have developed the CHSBS formalism to non-perturbatively compute the Fermion-Fermion scattering vertex for the case where the carrier Boson is initialized in an arbitrary quantum state.

In this Section and in the remainder of this manuscript, we will focus on a specific example, where a particular non-relativistic version of QED is realized by confining light within a material. This is currently experimentally achieved both with electrons in solid state [3, 4] and with synthetic materials made of ultracold atomic gases [2]. The confinement of light (for instance via mirrors forming a cavity) has two consequences which make these platforms ideal for exploring the phenomenology of interest. First, it allows to separate certain modes from the electromagnetic continuum and selectively couple them to the Fermions. Second, it enhances the QED coupling so that the equivalent of the fine-structure constant can become so large that already low intensity light (and even electromagnetic vacuum fluctuations) can affect a finite density of Fermions. Therefore, standard quantum optics techniques become available for preparing desired non-classical and non-Gaussian states of a small number of pho-

tons in few selected modes, also including spatial modes [5–7]. This allows to explore how carrier-state preparation affects the photon-mediated interactions and, since Fermions have fixed and controllable density, also collective phenomena like instabilities toward macroscopically ordered states.

In general, the above regime of QED within materials is an exciting playground for the study of collective phenomena, and several directions have emerged both for the solid-state [4] and ultracold-gas implementation [2]. While our CHSBS approach is not limited to a certain class of collective phenomena, we will here consider the case of photon-mediated pairing and the resulting instability toward a superconducting phase of the Fermions [23–27]. Recent works have studied various properties peculiar to this type of pairing, which is characterized by the fact that the photon-mediator has a gapped spectrum (due to the cavity mirrors) and at the same time is, at the relevant energies, very delocalized over the material or, equivalently, localized within a narrow region in momentum space, the latter being much smaller than the Fermi momentum for the solid-state realizations, but not necessarily for ultracold atoms. The peculiar properties revealed in these studies emerged already within the standard BCS-type approximation, where the photons adiabatically follow the Fermion dynamics, so that they effectively mediate a static interaction [23]. In particular, for certain Hubbard-type models, it has been shown that the sign of the interaction can be different if the photons are assumed to be in pure Fock states [29].

In a recent work [22], we showed however that the spatially delocalized cavity photons can mediate an additional, non-BCS type of resonant pairing. Here the Fermions fully absorb (or emit) a photon at its own characteristic cavity frequency. These resonant pairing processes can be dominant over BCS-type processes and are of a completely different nature. As we shall show in the next Section, these processes are the ones that depend on the quantum state of the mediator photon and generate the additional structure characterizing the CHSBS when the photon is prepared in non-Gaussian states.

A. Pairing-vertex function mediated by cavity photons

Here we will derive the CHSBS equation for the vertex function in the pairing channel and the mediator photon prepared in an arbitrary initial quantum state. Our model for QED consists of Fermions with dispersion ϵ_k (measured from the Fermi surface with energy E_F and momentum k_F), coupled to photons in a single standing-wave electromagnetic mode of the cavity with wavevector \vec{q}_0 and resonance frequency δ_c . This allows to express the Yukawa interaction Hamiltonian given in Eq.(24) in the momentum basis as:

$$H_{\text{light-matter}} = \sqrt{2\delta_c} \sum_{\vec{k}, \sigma} \sum_{\vec{q}=\pm q_0 \hat{x}} g_0 c_{\vec{k}+\vec{q}, \sigma}^\dagger c_{\vec{k}, \sigma} X. \quad (39)$$

We note that, while as in the standard QED the fundamental coupling is always between photons and the Fermion current (minimal coupling), we are considering here a coupling involving the Fermion density. We choose this variation because of two reasons. First, it can be experimentally realized using laser-assisted two-photon transitions both for electrons in solid state materials [24, 34] and ultracold fermionic atoms [2]; it also takes the same form if the photons are replaced by collective degrees of freedom, like lattice phonons [35] or Bogoliubov modes in a condensate [12], as realizable both in charge tuneable monolayer semiconductors [11] or ultracold Bose-Fermi mixtures [13, 14]. Second, it simplifies the momentum structure of the Yukawa coupling and thus the analysis of the vertex function. With these implementations in mind, the photon characteristic frequency δ_c is not the absolute value of the cavity resonance frequency but rather its de-

tuning from the laser frequency. A further advantage of these implementation is indeed the tuneability of the Hamiltonian via the laser parameters, not only its frequency but also the value of the Yukawa coupling constant g_0 , which is experimentally tuneable by the intensity of the laser beam. Finally, the coupling of the Fermions to a single standing-wave electromagnetic mode directly applies to the nanoplasmonic splitting cavities used in the solid-state implementations [24], as well as to the Fabry-Perot cavities used in the atomic-gas implementations [2]. Moreover, as discussed in Ref.22, as long as the characteristic photon momentum satisfies $q_0 \ll k_F$, which we will assume throughout, our treatment of the momentum structure of the vertex function does also apply to the coupling of the Fermions to a continuum of transverse cavity modes, as realized in solid-state microcavities [23] or in the atomic-gas context using confocal cavities [36].

For the specific QED model of Eq. (39), we obtain the effective action (27) describing the Fermion-Fermion interactions mediated by the photons, with the momentum-dependent coupling taking the simple form $V^{(0)}(\vec{q}) = g_0^2 \delta_c \delta_{\vec{q}, \pm \vec{q}_0}$. The equation for the intermediate, u -dependent vertex function (30), now written by making the Keldysh structure explicit, reads (we refer to the Appendix B for more details on the derivation)

$$\Gamma(u) = V^{(0)} D_A + M_{\text{BCS}} \circ \Gamma(u) + \frac{1+u}{1-u} M_{\text{res}} \circ \Gamma(u), \quad (40)$$

where we defined the matrix-multiplication in momentum-frequency space as $M \circ \Gamma(u) \equiv \int \frac{d\vec{k}}{(2\pi)^d} \frac{d\omega_1}{2\pi} M(\vec{p}\omega, \vec{k}\omega_1) \Gamma(\vec{k}, \omega_1; u)$, and with the matrices

$$\begin{aligned} M_{\text{BCS}}(\vec{p}\omega, \vec{k}\omega_1) &= \mathbf{i}V^{(0)}(\vec{k} - \vec{p}) \left[D_A(\omega_1 - \omega) G_K(\vec{k}, \omega_1) G_R(-\vec{k}, -\omega_1) + D_R(\omega_1 - \omega) G_R(\vec{k}, \omega_1) G_K(-\vec{k}, -\omega_1) \right] \\ M_{\text{res}}(\vec{p}\omega, \vec{k}\omega_1) &= \mathbf{i}V^{(0)}(\vec{k} - \vec{p}) 2\text{iIm} [D_R(\omega_1 - \omega)] G_R(\vec{k}, \omega_1) G_R(-\vec{k}, -\omega_1) \end{aligned} \quad (41)$$

defining the coupling between the different momentum and frequency components of the vertex function. We note that the two-particle vertex function $\Gamma(P, p, p')$ is in general a function of the COM coordinates $P = (\vec{P}, \Omega)$, incoming relative coordinates $p = (\vec{p}, \omega)$ and the outgoing relative coordinates $p' = (\vec{p}', \omega')$. However, Eq. (40), written in the pairing channel as per Eq.(41) (corresponding to choosing the two Fermion-lines in the Feynman diagram of Fig. 2 and 5 to be co-propagating), is a coupled equation only in the relative incoming coordinates, i.e. $\Gamma(P, p, p')$ couples to $\Gamma(P, k, p')$ and the kernel M within the ladder approximation is independent of p' . Moreover, since we want to study the superconducting instability we set $P = 0$ and express the vertex function in the simpler notation $\Gamma(\vec{p}, \omega) = \Gamma(P = 0, p, p')$, which describes the scattering of two Fermions with opposite spin, as well as with equal and opposite momenta and frequency (\vec{p}, ω) and $(-\vec{p}, -\omega)$. Here we restricted our calculation only to those initial density matrices of the photons which keep the

dynamics time-translation invariant (see discussion in Section V), which allowed us to write the equation (40) in frequency space.

The frequency-momentum and causal structure of Eq. (40) at thermal equilibrium has been discussed in Ref. 22, and we limit ourselves to review the main features below, in order to leave space for the discussion of the emergent Hilbert-space structure we focus on here. Let us first consider the second term on the R.H.S. of Eq. (40), containing M_{BCS} . It comes from the non-resonant processes discussed in the previous section and, as expected, it does not carry information about the initial state of the carrier. As we shall see next, it leads to the standard BCS scenario. It can be understood as two Fermions interacting via a retarded/advanced potential, whose frequency-dependence is set by the Fourier transform of the corresponding photon GF given in the second line of Eq.(23): $D_{R(A)}(\omega_1 - \omega) = 1/[2(\omega_1 - \omega \pm \text{i}0^+)^2 - 2\delta_c^2]$. Such pairing processes thus need the presence of Fermions,

whose distribution is thermal and encoded in the Fourier transform of the Keldysh GF of Eq. (9). For the sake of simplicity of the momentum structure, we start by considering the case of the cavity momentum $q_0 = 0$. In this non-resonant processes, Fermions always remain in the vicinity of the Fermi surface with momentum $\vec{p} \sim \vec{k} = \vec{k}_F$. We also assume that the Fermion distribution function is broadened by the finite lifetime of the quasi-particles as

$$G_K(\vec{k}, \omega_1) = \frac{1}{\omega_1 - \epsilon_{\vec{k}} - \mathbf{i}\tau^{-1}} \frac{[-2\mathbf{i}\tau^{-1} \tanh(\frac{\omega_1}{2T})]}{\omega_1 - \epsilon_{\vec{k}} + \mathbf{i}\tau^{-1}}.$$

This function has a pole in frequency at the characteristics energy scale of the Fermions near the FS $\omega_1 \sim \mathbf{i}\tau^{-1}$ in M_{BCS} of Eq. (41). Assuming that the photon gap is large: $\delta_c \gg \tau^{-1}$, and considering only the strongest pairing which happens in the limit of vanishing incoming relative frequency ω , the frequency dependence of the retarded interaction potential mediated by photons can be neglected, resulting in the usual static attractive interaction characterizing the BCS scenario. The vertex function of the low energy Fermions which form pairs under the attractive interaction defines the on-shell vertex function $\Gamma_{\text{on-shell}}(u) = \Gamma(|\vec{p}| \sim k_F, \omega \sim 0; u) \approx \Gamma(|\vec{p}| \sim k_F, \omega \sim \mathbf{i}\tau^{-1}; u)$. This identification to a single component $\Gamma_{\text{on-shell}}$ is valid as long as $\tau^{-1} \ll \delta_c$. In the case of finite cavity momentum $q_0 \ll k_F$, BCS processes couple the vertex function of the low-energy Fermions in the vicinity of the FS at momenta $|\vec{p}| \sim k_F, k_F \pm q_0$ and $\omega \sim 0, \epsilon_{k_F \pm q_0}$. Again, $\epsilon_{k_F \pm q_0} \ll \delta_c$ we can identify all the components of the vertex function within this small energy and momentum shell around FS as a single component $\Gamma_{\text{on-shell}}$, so that M_{BCS} becomes a diagonal matrix, coupling $\Gamma_{\text{on-shell}}(u)$ to itself.

The situation is different for the resonant processes encoded in M_{res} . The fact that these involve the full absorp-

tion/emission of a photon is formally expressed by the presence of

$$2\mathbf{i}\text{Im}D_R(\omega_1 - \omega) = \frac{-\pi\mathbf{i}}{2\delta_c} [\delta(\omega_1 - \omega - \delta_c) - \delta(\omega_1 - \omega + \delta_c)],$$

which is peaked at the cavity resonance frequency. As expected, these are the processes that carry the information about the initial state of the carrier in Eq. (40). These processes are non-diagonal in the frequency space of the vertex function, since a resonant photon scatters the incoming on-shell electrons ($\omega \sim 0$) to energies far away from the FS: $\omega_1 \sim \pm\delta_c$.

Using the Fourier transform of the retarded/advanced Fermion GF: $G_{R(A)}(\vec{k}, \omega) = 1/(\omega - \epsilon_{\vec{k}} \pm \mathbf{i}\tau^{-1})$, Eq. (40) becomes (see Appendix B for more details)

$$\Gamma_{\text{on-shell}}(T; u) = \Gamma_0 + \frac{2\tilde{g}\delta_c}{T}\Gamma_{\text{on-shell}}(u) - \tilde{g} \left[\Gamma(\vec{k}_F, \delta_c; u) + \Gamma(\vec{k}_F, -\delta_c; u) \right] \quad (42)$$

Here $\tilde{g} = g_0^2/(4\pi\delta_c)^2$ and the bare vertex $\Gamma_0 = V^{(0)}(\vec{k} - \vec{p})D_{0A}(\omega_1 - \omega) \approx -g_0^2/(2\delta_c)$.

In order to efficiently pair, the off-shell electrons have to undergo a second scattering process involving a resonant photon which brings them back to the on-shell region close to the FS. To compute this second-order process, one first uses Eq. (40) to find the first off-shell component of the vertex $\Gamma(\vec{k}_F, \pm\delta_c; u)$ as a function of the on-shell component only, which is done by neglecting the coupling to higher off-shell components. One then substitutes the result for $\Gamma(\vec{k}_F, \pm\delta_c; u)$ into Eq. (42) (this truncation is allowed for large photon gap [22]).

This yields the following closed equation for the on-shell component of the intermediate vertex function:

$$\Gamma_{\text{on-shell}}(T; u) = \Gamma_0 + \frac{\tilde{g}\delta_c}{T}\Gamma_{\text{on-shell}}(u) + 2 \left(\frac{\tilde{g}\delta_c}{\tau^{-1}} \right)^2 \left(\frac{1+u}{1-u} \right)^2 \Gamma_{\text{on-shell}}(u). \quad (43)$$

In the case when the carrier photon is initialized in a thermal Gaussian state, the above equation holds directly for the physical u -independent vertex function, whereby the fraction involving u appearing in the last term is substituted by the photon distribution function (see Eq. (47)). This thermal situation has by itself interesting properties which have been discussed in a previous work [22]. Here we limit ourselves to repeating that the second term on the R.H.S. represents the standard BCS contribution, where the polynomial dependence on T is due to the delocalized nature of the photons i.e. the delta-peak of the momentum-dependent coupling function $V^{(0)}(\vec{p})$. On the other hand, the third term on R.H.S. results from the resonant pairing processes, which carry the information about the initial carrier state via the source u . We note that, although the resonant pairing is a second-order process involving scattering

to the off-shell frequency sector and back, the small energy denominator ($\sim \tau^{-1}$) set by the characteristics energy scale of the low energy electrons can make it dominate over the BCS processes. The fact that the repeated absorption and emission of full photons remains resonant is due to the narrow cavity resonance together with the delocalized nature of the photons thanks to which the transfer a well-defined momentum. Even though the above equation for the intermediate vertex function has a closed form in frequency- and momentum-space, the explicit presence of the source u generates an additional structure in the equation for the physical vertex function. We demonstrated this for the general case of Section V, and in the next Section we will see this structure emerging for the specific pairing scenario considered here.

B. Photons prepared in a pure Fock state

We now focus on the case where the carrier photons are initially prepared in a pure Fock state described by the density matrix $\hat{\rho}_0 = |n\rangle\langle n|$. This can be achieved with many different protocols, and the most suitable one for the present purpose will depend on the specific realization of our QED within materials. Here we limit ourselves to observe that the possible strategies can be divided in two classes: i) a suitable light source is used to inject the photon Fock state inside the cavity, or ii) the photon Fock state is directly prepared inside the cavity. For the first class, sources of non-classical states of structured light are already available and being continuously developed [5–8], the additional step required for our purposes being the in-coupling of the light pulse into the cavity modes to which the matter couples. For the second class, several options exist which rely on coupling the desired cavity modes with some material degree of freedom inside the cavity. In the case where our QED model is implemented using atomic

gases, the additional degree of freedom can be for instance an internal electronic transition with a laser-assisted coupling to the cavity modes of interest (see e.g. [37]). This laser is then to be turned off after the state preparation, then another laser is used to dispersively couple the atomic motion to the cavity modes for the implementation of the QED coupling of Eq.(39). On the other hand, for solid-state implementations of our QED model, a piece of nonlinear medium can be added to the intracavity heterostructure, to which also the material hosting the quantum matter belongs. The coupling to the nonlinear medium can be then controlled by further driving lasers, as considered for instance in recent promising schemes [38]. An analogue situation can be realized with ultracold atoms, where the additional nonlinearity is brought in by a micromechanical element coupled to the cavity [39, 40].

Our goal is to compute the corresponding physical on-shell vertex function, which we denote by $\Gamma_{\text{on-shell}}^n$. Following the procedure illustrated in Eq.(32) for the general case, we derive the equation for $\Gamma_{\text{on-shell}}^n$ from the intermediate u -dependent vertex function $\Gamma_{\text{on-shell}}(u)$ given in Eq.(43). We obtain

$$\Gamma_{\text{on-shell}}^n(T) = \Gamma_0 + \frac{\tilde{g}\delta_c}{T}\Gamma_{\text{on-shell}}^n + 2\left(\frac{\tilde{g}\delta_c}{\tau^{-1}}\right)^2 \left[\Gamma_{\text{on-shell}}^n + 4 \sum_{m=0}^{n-1} (n-m)\Gamma_{\text{on-shell}}^m \right]. \quad (44)$$

As anticipated, despite the closed-form of the equation for the intermediate vertex $\Gamma_{\text{on-shell}}(T; u)$, the equation for the physical vertex $\Gamma_{\text{on-shell}}^n(T)$ is not closed. A new set of vertex components emerges, reflecting the Hilbert space structure of the initial quantum state of the photon carrier. As we have seen also in the general case of Section V, each of these additional components corresponds indeed to a given Fock state, with a number of photons lower than the initial photon number. Physically, this implies that the Fermion-Fermion vertex mediated by the carrier prepared in a pure Fock state with a given number of photons, effectively involves scattering processes mediated by all Fock states with a smaller number of resonant photons, down to the vacuum state. These scattering processes take place in different Hilbert space sectors of the carrier photon, and are organized hierarchically (as noted already in the general case of Eq.(34)), which means we can obtain the physical vertex $\Gamma_{\text{on-shell}}^n(T)$ in an iterative way starting from the vacuum state. The hierarchy is expressed in terms of the bare vertex Γ_0 and the function $M_{\text{vac}}(T) = \tilde{g}\delta_c/T + 2(\tilde{g}\delta_c)^2/(\tau^{-1})^2$. The latter is a combination of the entries of the matrix $M_{\text{BCS}} + M_{\text{res}}$, which governs the coupling between the different momentum-frequency

components of the vertex. The iterative solution then reads

$$\begin{aligned} \Gamma_{\text{on-shell}}^0(T) &= \frac{\Gamma_0}{1 - M_{\text{vac}}}, \\ \Gamma_{\text{on-shell}}^1(T) &= \Gamma_0 \left[\frac{1}{1 - M_{\text{vac}}} + \frac{1}{(1 - M_{\text{vac}})^2} \right], \\ \Gamma_{\text{on-shell}}^2(T) &= \Gamma_0 \left[\frac{1}{1 - M_{\text{vac}}} + \frac{3}{(1 - M_{\text{vac}})^2} + \frac{1}{(1 - M_{\text{vac}})^3} \right] \\ &\vdots \\ &\vdots \end{aligned} \quad (45)$$

At this point we can already note that as n increases $\Gamma_{\text{on-shell}}^n(T)$ shows a stronger divergence near $M_{\text{vac}}(T) = 1$, which corresponds to the pairing instability point i.e. the critical point of the transition towards a superconducting state. This leads to exotic critical behaviour near the superconducting transition, when the photons are initialized in different Fock states. This will be discussed in detail in Sec. VII.

C. Photons in thermal equilibrium with electrons

As done for the general case in Section VB, we will compute here the vertex function for the thermal case starting from the CHSBS equation. When the photons are initialized in a Gaussian thermal state at temperature $T = 1/\beta$ equal to the one of the electrons, the on-shell vertex function satisfies the following equation,

$$\begin{aligned}\Gamma_{\text{on-shell}}^{\text{th}}(T) &= \frac{1}{\sum_{n=0}^{\infty} e^{-\beta n \delta_c}} \sum_{n=0}^{\infty} e^{-\beta n \delta_c} \Gamma_{\text{on-shell}}^n, \\ &= \Gamma_0 + \frac{\tilde{g}\delta_c}{T} \Gamma_{\text{on-shell}}^{\text{th}} + 2 \left(\frac{\tilde{g}\delta_c}{\tau-1} \right)^2 \left[\Gamma_{\text{on-shell}}^{\text{th}} + \frac{4}{\sum_{n=0}^{\infty} e^{-\beta n \delta_c}} \sum_{n=0}^{\infty} e^{-\beta n \delta_c} \sum_{m=0}^{n-1} (n-m) \Gamma_{\text{on-shell}}^m \right],\end{aligned}\quad (46)$$

where in the last equation we have substituted $\Gamma_{\text{on-shell}}^n(T)$ from Eq.(44). As we discussed in Section VB, we can further organize the last term on the R.H.S. of the above equation by collecting coefficients of $\Gamma_{\text{on-shell}}^m(T)$ in the infinite series to obtain a closed-form equation in terms of $\Gamma_{\text{on-shell}}^{\text{th}}$,

$$\Gamma_{\text{on-shell}}^{\text{th}}(T) = \Gamma_0 + \left[\frac{\tilde{g}\delta_c}{T} + 2 \left(\frac{\tilde{g}\delta_c}{\tau-1} \right)^2 \coth^2 \left(\frac{\delta_c}{2T} \right) \right] \Gamma_{\text{on-shell}}^{\text{th}}(T).\quad (47)$$

Instead of the Fock-state hierarchy of equations given in Eq. (45) containing $M_{\text{vac}}(T)$, we obtain here a single equation containing $M_{\text{th}}(T) = \tilde{g}\delta_c/T + 2(\tilde{g}\delta_c/\tau-1)^2 \coth^2(\delta_c/2T)$. As seen in the general case, this is possible since the thermal Gaussian state allows for a rearrangement of the Hilbert-space structure of the scattering such that the latter becomes irrelevant, and the equation for the on-shell vertex function can be directly closed.

VII. CRITICAL PROPERTIES OF SUPERCONDUCTING TRANSITION

In the previous Section, we have computed the two-particle scattering vertex function for electrons interacting via photons according to the QED model of Eq.(39). Being interested in the superconducting phase transition, we computed the scattering in the pairing channel. As we have seen, within the standard BCS approximation, cavity photons mediate a static, attractive interaction potential, provided that the detuning of the cavity resonance frequency is positive ($\delta_c > 0$). This attractive interaction is further enhanced by the non-BCS processes involving absorption and emission of resonant photons owing to the long-range nature of the interaction. At the critical temperature for the superconducting transition, the vertex function in the pairing channel diverges, indicating an instability towards the formation of two-particle bound states, i.e., Cooper pairs with opposite momentum and spin [15]. In this Section, we will use the CHSBS formalism to study the critical properties of the superconducting transition, comparing the case where the photon is in a thermally mixed Gaussian state at equilibrium with the electrons, with the case where it is prepared in a pure Fock state.

With this aim, we introduce the pairing field $\Delta^P(p)$ (also known as superconducting gap field), which is in general a function of the coordinates of both electrons in the pair, or equivalently of both the relative p and the COM coordinate P (see Section VIA). It can be used as an auxiliary field to decouple the quartic electron-electron interaction term S_{eff} in Eq.(27) into a form which is diagonal in the the COM coordi-

nate:

$$e^{\text{i}S_{\text{eff}}} = \prod_P \int D[\Delta^P(p)] e^{\text{i} \int dp dp' \Delta^{P*}(p) \Gamma_0^{-1}(p,p';u) \Delta^P(p')} \times e^{\text{i} \int dp \Delta^P(p) \psi^*(P+p) \psi^*(P-p) + h.c.}.\quad (48)$$

Here $\Gamma_0^{-1}(p, p'; u) = 1/V^{(0)}(\vec{p}' - \vec{p})D(\omega' - \omega; u)$. This procedure, known as Hubbard-Stratonovich decoupling [31, 41], is a property of Gaussian path integrals. The resulting action is quadratic in the fermionic fields ψ , which can thus be integrated out exactly to get an action $S(\Delta; u)$ solely in terms of the pairing field. Up to quadratic order, this action reads

$$e^{\text{i}S_{\text{eff}}} = \prod_P \int D[\Delta^P(p)] e^{\text{i} \int dp dp' \Delta^{P*}(p) \Gamma^{-1}(P,p,p';u) \Delta^P(p')},\quad (49)$$

where $\Gamma(P, p, p'; u)$ is the u -dependent two-particle vertex function introduced in the previous Section. From the action (49), we see that it corresponds to the Gaussian GF of the pairing field $\Delta^P(p)$. The physical two particle vertex function $\Gamma(P, p, p')$ (and thus the physical pair GF) corresponding to a given initial density matrix $\hat{\rho}_0$ of the mediator photon is then obtained from $\Gamma(P, p, p'; u)$ through the proper set of u -derivatives described in the previous Sections. Next, we will analyze the pair GF $\Gamma(P, p, p')$, computed via the CHSBS formalism, at and in the vicinity of the transition point, in order to extract some of the critical properties.

A. Critical temperature

At the critical point, the low energy electrons having zero COM momentum and frequency ($P = 0$), as well as relative coordinates at FS ($|\vec{p}'| \approx k_F, \omega \approx 0$) become unstable towards pair formation. This is manifested as a pole in the on-shell two-particle vertex function $\Gamma_{\text{on-shell}}(T) = \Gamma(P = 0; |\vec{p}'| \approx k_F, \omega \approx 0; p')$ at $T = T_c$, associated with a uniform pairing field $\Delta^{P=0}(p = 0)$. In this sub-Section, we will calculate the critical temperature using $\Gamma_{\text{on-shell}}(T)$ obtained in Section VI.

We first consider the equilibrium case where the photons are initialized in a thermal and Gaussian density matrix at a temperature T equal to that of the electrons. In this case, the physical on-shell vertex function $\Gamma_{\text{on-shell}}^{\text{th}}$ given in Eq.(47) diverges when $M_{\text{th}}(T) = 1$, yielding the equation of the critical temperature:

$$\frac{\tilde{g}\delta_c}{T_c^{\text{th}}} + 2 \left(\frac{\tilde{g}\delta_c}{\tau^{-1}} \right)^2 \coth^2 \left(\frac{\delta_c}{2T_c^{\text{th}}} \right) = 1. \quad (50)$$

We discussed the solution of the above equation for T_c^{th} in Ref.22, considering a Fermi-liquid type lifetime of electrons due to the screened Coulomb interaction $\tau^{-1}(T) = (\pi T^2/8E_F) \log(E_F/T)$. For realistic parameters in 2D materials (STO/LAO) coupled to a tera-Hertz split-ring cavity, the superconducting transition in the thermal case occurs in the low Kelvin regime. We note that the photon resonance frequency in these cavities satisfies $\delta_c \gg T_c$, so that the average number of photons in the cavity is negligible: $\langle \hat{n} \rangle = 0.5 \coth \left(\frac{\delta_c}{2T_c^{\text{th}}} \right) - 0.5 \sim 0$. The critical temperature in this vacuum case can be calculated from,

$$T_c^{\text{vac}} = \frac{\tilde{g}\delta_c}{1 - 2 \left(\frac{\tilde{g}\delta_c}{\tau^{-1}} \right)^2}. \quad (51)$$

It is however important to note, that the actual critical temperature in the thermal equilibrium case, though very close to T_{vac} , is always going to be slightly larger due to the average number of photons not being exactly zero.

We now turn our attention to the case of photons prepared in a Fock state, $\hat{\rho}_0 = |n\rangle\langle n|$. The corresponding on-shell physical vertex function $\Gamma_{\text{on-shell}}^n$ satisfies Eq.(44). As evident from the iterative solution for $\Gamma_{\text{on-shell}}^n$ given in Eq.(45), for any finite photon number n in the Fock state, $\Gamma_{\text{on-shell}}^n$ diverges when the denominator $M_{\text{vac}} = 2\tilde{g}\delta_c/T + 32(\tilde{g}\delta_c)^2/(\tau^{-1})^2$ approaches to 1. This implies that the superconducting transition occurs at the same critical temperature T_c^{vac} as the thermal vacuum case, independently of the number of photons in the Fock state.

B. Susceptibility exponent

Since Γ is equivalent to the propagator of the pairing field, the exponent characterizing the divergence of $\Gamma_{\text{on-shell}}(T - T_c)$ as T approaches T_c corresponds to the critical susceptibility exponent γ :

$$\Gamma_{\text{on-shell}}(T - T_c) \sim \frac{1}{|T - T_c|^\gamma}. \quad (52)$$

We again first consider a Gaussian thermal initial state of the mediator photons. In this case, $\Gamma_{\text{on-shell}}^{\text{th}}$ given in Eq.(47) diverges when $M_{\text{th}}(T = T_c^{\text{th}}) = 1$ (see Eq.(50)). In the regime of interest $T \ll E_F$, $M_{\text{th}}(T) = \tilde{g}\delta_c/T + 2(\tilde{g}\delta_c/\tau^{-1})^2 \coth^2(\delta_c/2T)$ (including the temperature dependent life-time of the quasi-particles) is a smooth function

of T . Hence, in order to analyze the nature of the singularity in $\Gamma_{\text{on-shell}}^{\text{th}}$, we can expand $M_{\text{th}}(T)$ in a Taylor's series around $T = T_c^{\text{th}}$, to obtain

$$\Gamma_{\text{on-shell}}^{\text{th}} \propto \frac{\Gamma_0}{T - T_c^{\text{th}}}. \quad (53)$$

This yields $\gamma = 1$, which recovers the standard BCS result of the susceptibility critical exponent for the Gaussian fixed point in thermal equilibrium. That is, when the mediator photon is initialized in a Gaussian thermal state, the superconducting transition temperature is strongly modified by the non-BCS resonant pairing processes (see Section VIA), but the critical behaviour of the pairing susceptibility remains unaltered from the standard BCS case.

We now turn to the case where the mediator photon is initialized in a Fock state. For Fock states with any finite number of photons n , $\Gamma_{\text{on-shell}}^n$ given in Eq.(44) always diverges at the vacuum critical temperature T_c^{vac} , defined by $M_{\text{vac}}(T = T_c^{\text{vac}}) = 1$. As apparent from Eq. (45), in the vicinity of the phase transition, the strongest divergence in $\Gamma_{\text{on-shell}}^n$ comes in the form,

$$\Gamma_{\text{on-shell}}^n \sim \frac{\Gamma_0}{(1 - M_{\text{vac}}(T))^{n+1}} \propto \frac{\Gamma_0}{(T - T_c^{\text{vac}})^{n+1}}, \quad (54)$$

where we expanded M_{vac} in Taylor's series around the critical temperature T_c^{vac} . This yields the susceptibility exponent $\gamma = n + 1$. That is, while the critical temperature remains unaffected, the critical behaviour is dramatically altered, as the critical exponent becomes linearly proportional to the number of photons prepared in the Fock state.

C. Correlation-length exponent

Finally, we study the critical behaviour of the spatial correlations of the pairing field $\Delta(\vec{r})$, defined as,

$$\langle \Delta(\vec{r}_1) \Delta^*(\vec{r}_2) \rangle = \int \int \frac{d\vec{P}}{(2\pi)^d} \frac{d\vec{p}}{(2\pi)^d} \langle \Delta^{\vec{P}}(\vec{p}) \Delta^{\vec{P}*}(-\vec{p}) \rangle \times e^{i\vec{P} \cdot (\vec{r}_1 - \vec{r}_2) + i\vec{p} \cdot (\vec{r}_1 + \vec{r}_2)}. \quad (55)$$

Near the phase transition, the above integral is dominated by the contribution coming from $\vec{P} \approx 0$ and $\vec{p} = \vec{k}_F$, since the divergent component of the pair GF is $\Gamma(\vec{P} = 0, \Omega = 0, \vec{p} = \vec{k}_F, \omega = 0, p')$. In order to obtain the long-distance behaviour of the correlation function with spatial separation $|\vec{r}_1 - \vec{r}_2|$, we expand $\Gamma(\vec{P}, \Omega = 0, \vec{p} = \vec{k}_F, \omega = 0, p')$ in Taylor's series around $\vec{P} = 0$ and $T = T_c$ to the lowest non-trivial order. Near the critical point, the spatial correlation decays exponentially $\sim \exp(-|\vec{r}_1 - \vec{r}_2|/\xi(T))$ with a characteristic correlation length $\xi(T) \sim (T - T_c)^{-\nu}$. $\xi(T)$ diverges at $T = T_c$ with the critical exponent ν and the system becomes scale-invariant at the phase transition.

Again, we first consider the mediator photons being prepared in a Gaussian thermal state. In this case, the physi-

cal two-particle vertex function $\Gamma^{\text{th}}(\vec{P}, \Omega = 0, \vec{p} = \vec{k}_F, \omega = 0, p') = \tilde{\Gamma}^{\text{th}}(\vec{P}, T)$, expanded around $\vec{P} = 0$ and $T = T_c^{\text{th}}$, reads (to leading order)

$$\tilde{\Gamma}^{\text{th}}(\vec{P}, T) = \frac{\Gamma_0}{P^2 (\cos^2 \theta + a) + m(T - T_c^{\text{th}})}. \quad (56)$$

Here θ is the angle between the COM momentum \vec{P} measured from the relative momentum of the incoming electrons $\vec{p} = \vec{k}_F$ and a is a constant (independent of \vec{P} and T) depending on the characteristic energy scales of the electrons and photons at $T = T_c^{\text{th}}$. $m(T - T_c^{\text{th}}) \propto (T - T_c^{\text{th}})$ is the mass gap obtained by expanding $M_{\text{th}}(T)$ upto linear order around $T = T_c^{\text{th}}$ (see Eq.(53)). The above form of $\tilde{\Gamma}^{\text{th}}(\vec{P}, T)$ can be obtained analytically, by Taylor expansion of $\tilde{\Gamma}^{\text{th}}(\vec{P}, T)$ around $\vec{P} = 0$ and $T = T_c^{\text{th}}$. Here we motivate this form by general symmetry arguments. In the scattering events contributing to in $\tilde{\Gamma}^{\text{th}}(\vec{P}, T)$, two incoming electrons close to the FS and having momentum $\vec{P} + \vec{k}_F$ and $\vec{P} - \vec{k}_F$, interact by exchanging cavity photons of momentum $\vec{q}_0 \approx 0$ and are scattered to the same momenta $\vec{P} \pm \vec{k}_F$ and $\vec{P} \mp \vec{k}_F$ near the FS. Since the photon momentum \vec{q}_0 fixed by the cavity singles out a direction, momentum conservation breaks the rotational symmetry of the scattering, making the scattering amplitude $\tilde{\Gamma}^{\text{th}}(\vec{P}, T)$ dependent on θ (unlike the standard case of phonon-mediated superconductivity). Still, inversion symmetry $\vec{P} \rightarrow -\vec{P}$ prohibits terms linear in \vec{P} (and hence in $\cos \theta$) to appear in the expansion of $\tilde{\Gamma}^{\text{th}}(\vec{P}, T)$.

To obtain the spatial correlation function, we then perform the Fourier transform,

$$\int \frac{d\vec{P}}{(2\pi)^d} \tilde{\Gamma}^{\text{th}}(\vec{P}, T) e^{i\vec{P} \cdot (\vec{r}_1 - \vec{r}_2)} \propto e^{-|\vec{r}_1 - \vec{r}_2| \sqrt{\frac{m(T - T_c^{\text{th}})}{1+a}}}. \quad (57)$$

This implies that the correlation length ξ diverges as,

$$\xi \propto \frac{1}{(T - T_c^{\text{th}})^{\frac{1}{2}}}, \quad (58)$$

that is, $\nu = \frac{1}{2}$. This correlation length exponent for photons prepared in a Gaussian thermal state is the same as in the standard BCS scenario.

We now finally consider photons initialized in a Fock state. The spatial behaviour of the correlation function is extracted from the physical vertex function $\Gamma^n(\vec{P}, \Omega = 0, \vec{p} = \vec{k}_F, \omega = 0, p') = \tilde{\Gamma}^n(\vec{P}, T)$ expanded the critical point $\vec{P} = 0, T = T_c^{\text{vac}}$. As for the thermal case, the functional dependence of $\tilde{\Gamma}^n(\vec{P}, T)$ on P^2 and θ is constrained by the symmetries of the problem, while the leading order temperature dependence comes from the expansion of $M_{\text{vac}}(T)$ around $T = T_c^{\text{vac}}$. However, the crucial difference from the thermal case lies in the polynomially stronger divergence of the Γ at the critical

point, leading to the following form

$$\begin{aligned} \tilde{\Gamma}^n(\vec{P}, T) &= \frac{\Gamma_0}{[P^2 (\cos^2 \theta + a) + m(T - T_c^{\text{vac}})]^{n+1}}, \\ &\approx \frac{1}{m^n (n+1)} \frac{\Gamma_0}{\left[P^2 (\cos^2 \theta + a) + \frac{m}{n+1} \right]}, \end{aligned} \quad (59)$$

where in the last equation we expanded the denominator in a binomial series and kept the lowest-order terms in P . We see that the temperature dependent mass gap $m(T - T_c^{\text{vac}})$ is now effectively reduced by a factor $n+1$, yielding an exponential decay of the spatial correlations of the form

$$\int \frac{d\vec{P}}{(2\pi)^d} \tilde{\Gamma}^n(\vec{P}, T) e^{i\vec{P} \cdot (\vec{r}_1 - \vec{r}_2)} \propto e^{-|\vec{r}_1 - \vec{r}_2| \sqrt{\frac{m(T - T_c^{\text{vac}})}{(1+a)(n+1)}}}. \quad (60)$$

Hence, the correlation length reads

$$\xi \propto \left(\frac{n+1}{T - T_c} \right)^{1/2}.$$

We thus see that, while the correlation-length exponent remains unaltered from the BCS case $\nu = 1/2$, the correlation length scales with the square root of the number of photons in the Fock state. This result completes the derivation of the critical properties summarized in Fig. 3.

VIII. POLARIZABILITY AND THE TIME-INDEPENDENT APPROXIMATION

So far, we have considered a time-independent situation in which the carrier photon remains in its initial quantum state. However, the latter is in principle affected by the interactions with the fermionic matter. In general, if our QED system of Fermions and photons would be ergodic, the whole system would thermalize and the memory of the initial photon state would be lost. In fact, the constraints imposed by gauge invariance can lead to ergodicity breaking through what is called disorder-free many-body localization [19, 20]. For our QED within materials, one can thus expect the memory of the initial state never to be lost completely. How this happens and what consequences it has for the present phenomenology is a very interesting fundamental question, that we defer however to future investigations.

Here we instead consider a different mechanism for the preservation of the memory of the initial photon state, which is simply the strong suppression of the effect of the material onto the photons [21]. This effect is described by the polarization function, $\Pi(\omega, q_0)$, where ω and q_0 are the energy and momentum of the photon. In our Keldysh formalism, the polarization function has two components: the retarded, $\Pi_R(\omega, q_0)$ and the Keldysh, $\Pi_K(\omega, q_0)$. The real part of $\Pi_R(\omega, q_0)$ modifies the dispersion of the photons, while its imaginary part, resulting from on-shell processes, introduces absorption. When the fermionic matter is in thermal equilibrium, the imaginary part of the polarization function fixes also the Keldysh component via a fluctuation dissipation relation:

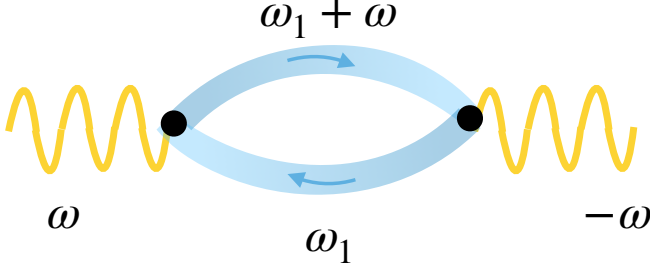


FIG. 6. Feynman diagram corresponding to the polarization function of the Fermions. It quantifies the backaction of the matter onto the light, and in particular the modification of the initial quantum state of the photon.

$\Pi_K(\omega, q_0) = 2i \coth(\omega/2T) \text{Im}[\Pi_R(\omega, q_0)]$. The Keldysh component is the relevant one here, as we are interested in the possible modification of the initial quantum state of the photons, which we have seen being encoded in the Keldysh GF.

As noted already above, a characteristic feature of the regime of QED considered here is the strong separation of energy and momentum scales between light and matter: compared to the fermionic scales, the cavity photons have a large energy gap $\delta_c \gg \epsilon_{k_F+q_0} (\approx v_F q_0)$ but at the same time very small momentum $q_0 \ll k_F$. Here v_F is the Fermi velocity. In the present model of QED, given in Eq. (39), the photons couple to the electron density, which is a conserved quantity. This fact, as we argue next, together with the above separation of scales, implies that the polarization function has to be small, thereby guaranteeing the preservation of the memory of the initial quantum state of the photon.

As shown in Ref. 42 for a general class of Yukawa couplings between a real Boson and Fermions, of which our QED coupling is a particular case, this result applies every time the interaction form factor is constant. Let us briefly repeat the general argument here. Let us first consider the zero-momentum case. $\Pi_R(\omega, 0)$ is the two-time correlator of the total number of electrons $n_f = \sum_{\vec{k}, \sigma} \psi_{\vec{k}, \sigma}^\dagger \psi_{\vec{k}, \sigma}$, the latter being conserved. The time-independence of n_f then results in $\Pi_R(\omega, 0) = 0$. By continuity one can then imply that $\Pi_R(\omega, q)$ has to remain small in the limit $\omega \gg v_F q$. This limit is exactly the limit of interest in our case where $\delta_c \gg v_F q_0$. We thus can conclude that the polarization function, whose leading-order diagrammatic expression is shown in Fig. 6, should be small compared to δ_c even when fully dressed with high-order corrections. In Ref. 42, this general argument has been verified both perturbatively and non-perturbatively.

We finally note that, in the regime of interest here where the polarization function remains small, phase transitions of the superradiant type, characterized by a macroscopic occupation of the cavity mode and a density modulation of the Fermions [36, 43–51], are excluded.

IX. CONCLUSIONS

In this work, we developed a field-theoretical framework for the study of the effect of carrier-quantum-state preparation on scattering and collective phenomena. We derived an equation for the two-particle scattering vertex for the case where the force carrier mediating the scattering is initially prepared in an arbitrary quantum state. This CHSBS equation is characterized by an additional structure in an emergent scattering space which adds to the standard energy-momentum space. This emergent scattering structure reflects the wave-function of the quantum state of the force carrier in Hilbert space, and is nontrivial when the latter is not Gaussian. Gaussian and in particular thermal Gaussian states of the mediator instead allow for a reorganization of the additional Hilbert-space structure that renders the latter irrelevant, yielding the standard Bethe-Salpeter equation for the scattering vertex. As a first example, we applied our CHSBS equation to the case of photon-mediated pairing and superconductivity for electrons in cavities, and showed that photons prepared in pure Fock states strongly enhance pair correlations and ultimately modify superconducting critical properties like the susceptibility exponent or the correlation length, which become dependent on the number of photons.

This work shows that by preparing the quantum state of a force carrier the properties of scattering and the resulting collective phenomena can be deeply altered. By developing a theoretical tool for the systematic investigation of this possibility, it paves the way for further investigations exploring new scenarios in few- and many-body physics. Several different research directions emerge naturally from the present work. For instance the study of the effect of other non-Gaussian non-classical states of the force carrier, beyond the Fock state on which we have focused here. Or the investigation of different ordering phenomena besides the pairing considered here, and how these can be manipulated by carrier-state preparation, including also (frustrated) magnetism with photon-mediated interactions [34, 52]. QED within materials also allows to address our central question from the complementary perspective where the electrons play the role of the force carriers of interactions between photons or polaritons [11, 12], for which a non-equilibrium field theory has been recently developed [53–56] that could be extended in the future to include the effect of the carrier-state preparation.

ACKNOWLEDGMENTS

We thank Martina Zündel for careful reading of the manuscript. AC acknowledges Abrahams Postdoctoral Fellowship by Rutgers Center for Material Theory where last part of the work is performed.

Appendix A: Complete expression of the effective action

In the main text, we formulated the CHSBS formalism to study Fermion-Fermion scattering mediated by exchange of

Bosons which are prepared in arbitrary non-thermal initial density matrices. As we discussed in section IV, the information about the initial conditions of the non-interacting system is incorporated by introducing a set of quadratic sources

$\{u_s\}$ coupled to the bi-linears of the initial fields and taking appropriate set of derivatives w.r.t. $\{u_s\}$ to compute physical correlation functions (or more generally physical partition function).

We considered the Fermion-Boson coupling to be a Yukawa-type interaction given by S_{int} in Eq.(25). Since the action $S_B + S_{\text{int}}$ is a quadratic action in Bosonic fields, we can integrate out the Bosonic fields X_{cl} and X_Q exactly to obtain an effective Fermion-Fermion action S_{eff} of the form (see Eq.(27) of the main text),

$$\begin{aligned}
S_{\text{eff}}(u) = & - \int \int dt dt' \sum_{\{k_i\}, s} V^{(0)}(\{k_i\}, s) \\
& \left[D_R(s, t, t') \left[\psi_{cl}^*(k_1, t) \{ \psi_{cl}^*(k_2, t') \psi_{cl}(k_3, t') + cl \leftrightarrow q \} \psi_q(k_4, t) \right. \right. \\
& \quad \left. \left. + \psi_q^*(k_1, t) \{ \psi_{cl}^*(k_2, t') \psi_{cl}(k_3, t') + cl \leftrightarrow q \} \psi_{cl}(k_4, t) \right] \right. \\
& + D_A(s, t, t') \left[\psi_{cl}^*(k_1, t) \{ \psi_{cl}^*(k_2, t') \psi_q(k_3, t') + cl \leftrightarrow q \} \psi_{cl}(k_4, t) \right. \\
& \quad \left. + \psi_q^*(k_1, t) \{ \psi_{cl}^*(k_2, t') \psi_q(k_3, t') + cl \leftrightarrow q \} \psi_q(k_4, t) \right] \\
& + D_K(s, t, t'; u) \left[\psi_{cl}^*(k_1, t) \{ \psi_{cl}^*(k_2, t') \psi_q(k_3, t') + cl \leftrightarrow q \} \psi_q(k_4, t) \right. \\
& \quad \left. + \psi_q^*(k_1, t) \{ \psi_{cl}^*(k_2, t') \psi_q(k_3, t') + cl \leftrightarrow q \} \psi_{cl}(k_4, t) \right] \left. \right]. \tag{A1}
\end{aligned}$$

Here the four-Fermion interaction is mediated by the Bosonic Green's functions $D(s, t, t'; u)$ where the Keldysh component $D_K(s, t, t'; u)$ solely carries the initial source dependence in the effective Fermionic theory.

The vertex functions corresponding to the 12 bare vertices shown in Eq.(A1) obey 12 equations which are coupled in Keldysh space. As discussed in Ref.[22], for the cavity-QED example given in section VIA, one of those 12 equations decouples from the others and is the relevant one to be considered.

Appendix B: Details of the derivation of pairing-vertex function mediated by cavity photons

This equation is written in Eq.(40) and (41) of the main text, and reads (in explicit form)

$$\begin{aligned}
& \Gamma(\vec{P}, \Omega; \vec{p}, \omega; \vec{p}', \omega'; u) = V^{(0)}(\vec{p}' - \vec{p}) D^A(\omega' - \omega) \\
& + \mathbf{i} \int \frac{d\vec{k}}{(2\pi)^2} \frac{d\omega_1}{2\pi} V^{(0)}(\vec{k} - \vec{p}) D_A(\omega_1 - \omega) G_K(\vec{P} + \vec{k}, \Omega + \omega_1) G_R(\vec{P} - \vec{k}, \Omega - \omega_1) \Gamma(\vec{P}, \Omega; \vec{k}, \omega_1; \vec{p}', \omega'; u) \\
& + \mathbf{i} \int \frac{d\vec{k}}{(2\pi)^2} \frac{d\omega_1}{2\pi} V^{(0)}(\vec{k} - \vec{p}) D_R(\omega_1 - \omega) G_R(\vec{P} + \vec{k}, \Omega + \omega_1) G_K(\vec{P} - \vec{k}, \Omega - \omega_1) \Gamma(\vec{P}, \Omega; \vec{k}, \omega_1; \vec{p}', \omega'; u) \\
& + \mathbf{i} \int \frac{d\vec{k}}{(2\pi)^2} \frac{d\omega_1}{2\pi} V^{(0)}(\vec{k} - \vec{p}) D_K(\omega_1 - \omega; u) G_R(\vec{P} + \vec{k}, \Omega + \omega_1) G_R(\vec{P} - \vec{k}, \Omega - \omega_1) \Gamma(\vec{P}, \Omega; \vec{k}, \omega_1; \vec{p}', \omega'; u). \tag{B1}
\end{aligned}$$

First, we will calculate the 2nd and the 3rd term of the R.H.S. of Eq.(B1) (referred as $M_{\text{BCS}} \circ \Gamma(u)$ in the main text) which lead to the standard BCS pairing processes involving adiabatic photons and on-shell electrons. As we discussed in the main text, in order to probe the superconducting instability we set $\vec{P} = 0, \Omega = 0$ and $\vec{p} = \vec{k}_F, \omega = 0$. Also for the sake of simplicity, we assume the cavity momentum $q_0 = 0$. This immediately simplifies the structure of the loop momentum integral over \vec{k} and just sets it to $\vec{k} = \vec{p} = \vec{k}_F$. The loop frequency integral over ω_1 is performed by the method of contour integration by choosing the pole of $G_K(\vec{k}_F, \omega_1)$ at $\omega_1 = \pm \mathbf{i}\tau^{-1}$. Hence the photonic retarded/advanced Green's functions are evaluated at frequencies $\omega_1 - \omega = \pm \mathbf{i}\tau^{-1}$ which is much smaller than photon resonance frequency δ_c . This is similar to the standard BCS picture where the Boson mediates a static attractive potential. This yields (for 2d electrons coupled to cavity photons),

$$\int \int d\vec{k} d\omega_1 M_{\text{BCS}}(\vec{p} = \vec{k}_F, \omega = 0; \vec{k}, \omega_1) \Gamma(\vec{k}, \omega_1; u) = \tilde{g} \delta_c \sum_{\omega_1 = \pm \mathbf{i}\tau^{-1}} \tanh \frac{\omega_1}{2T} \frac{1}{\omega_1} \Gamma(\vec{k}_F, \omega_1; u) = \frac{\tilde{g} \delta_c}{T} \Gamma_{\text{on-shell}}(u). \tag{B2}$$

Next, we will evaluate the resonant contribution given by the 4th term in Eq.(B1) on R.H.S. In the case, the delta functions in $D_K(\omega_1 - \omega; u)$ set the loop frequency variable $\omega_1 = \pm\delta_c$ to yield,

$$\begin{aligned} \int \int d\vec{k} d\omega_1 M_{\text{res}}(\vec{p} = \vec{k}_F, \omega = 0; \vec{k}, \omega_1) \Gamma(\vec{k}, \omega_1; u) &= \tilde{g}\delta_c^2 \sum_{\omega_1 = \pm\delta_c} G_R(\vec{k}_F, \omega_1) G_R(-\vec{k}_F, -\omega_1) \Gamma(\vec{k}_F, \omega_1; u) \\ &= -\tilde{g} \left[\Gamma(\vec{k}_F, \delta_c; u) + \Gamma(\vec{k}_F, -\delta_c; u) \right]. \end{aligned} \quad (\text{B3})$$

The above term makes the equation non-diagonal in frequency space, coupling $\Gamma_{\text{on-shell}}$ to the high-frequency component of the vertex function involving off-shell electrons scattered by resonant photons ($\omega_1 - \omega = \pm\delta_c$).

Now we need to evaluate the BCS components of the equation at the external frequency $\omega = \pm\delta_c$. This yields,

$$\int \int d\vec{k} d\omega_1 M_{\text{BCS}}(\vec{p} = \vec{k}_F, \omega = \pm\delta_c; \vec{k}, \omega_1) \Gamma(\vec{k}, \omega_1; u) \approx -\frac{\tilde{g}\delta_c^3}{2T} \sum_{\omega_1 = \pm i\tau^{-1}} \left[\frac{1}{\pm 2i\delta_c\tau^{-1}} \right] \Gamma(\vec{k}_F, \omega_1; u). \quad (\text{B4})$$

Hence,

$$\int \int d\vec{k} d\omega_1 \left[M_{\text{BCS}}(\vec{p} = \vec{k}_F, \omega = \delta_c; \vec{k}, \omega_1) + M_{\text{BCS}}(\vec{p} = \vec{k}_F, \omega = -\delta_c; \vec{k}, \omega_1) \right] \Gamma(\vec{k}, \omega_1; u) \approx 0. \quad (\text{B5})$$

The off-shell vertex component is thus given by (neglecting the contributions from further off-shell sectors like $\Gamma(\vec{k}_F, \pm 2\delta_c; u)$ [22])

$$\int \int d\vec{k} d\omega_1 M_{\text{res}}(\vec{k}_F, \delta_c; \vec{k}, \omega_1) \Gamma(\vec{k}, \omega_1; u) = \tilde{g}\delta_c^2 G_R(\vec{k}_F, 0) G_R(-\vec{k}_F, 0) \Gamma(\vec{k}_F, 0; u) \approx -\frac{\tilde{g}\delta_c^2}{\tau^{-2}} \Gamma_{\text{on-shell}}(u). \quad (\text{B6})$$

Substituting this in Eq.(B3), we obtain the closed-form equation for $\Gamma_{\text{on-shell}}(u)$ given in Eq. (43) of the main text.

-
- [1] D. F. Walls and G. J. Milburn, *Quantum optics* (Springer Science & Business Media, 2007).
- [2] F. Mivehvar, F. Piazza, T. Donner, and H. Ritsch, *Advances in Physics* **70**, 1 (2021), <https://doi.org/10.1080/00018732.2021.1969727>.
- [3] F. J. Garcia-Vidal, C. Ciuti, and T. W. Ebbesen, *Science* **373**, eabd0336 (2021).
- [4] F. Schlawin, D. M. Kennes, and M. A. Sentef, arXiv preprint arXiv:2112.15018 (2021).
- [5] H. Rubinsztein-Dunlop, A. Forbes, M. V. Berry, M. R. Dennis, D. L. Andrews, M. Mansuripur, C. Denz, C. Alpmann, P. Banzer, T. Bauer, E. Karimi, L. Marrucci, M. Padgett, M. Ritsch-Marte, N. M. Litchinitser, N. P. Bigelow, C. Rosales-Guzman, A. Belmonte, J. P. Torres, T. W. Neely, M. Baker, R. Gordon, A. B. Stilgoe, J. Romero, A. G. White, R. Fickler, A. E. Willner, G. Xie, B. McMorrin, and A. M. Weiner, *Journal of Optics* **19**, 013001 (2016), publisher: IOP Publishing.
- [6] A. Forbes and I. Nape, *AVS Quantum Science* **1**, 011701 (2019), publisher: American Vacuum Society.
- [7] Y.-S. Ra, A. Dufour, M. Walschaers, C. Jacquard, T. Michel, C. Fabre, and N. Treps, *Nature Physics* **16**, 144 (2020).
- [8] M. Erhard, M. Krenn, and A. Zeilinger, *Nature Reviews Physics* **2**, 365 (2020).
- [9] Y. Chu, P. Kharel, T. Yoon, L. Frunzio, P. T. Rakich, and R. J. Schoelkopf, *Nature* **563**, 666 (2018).
- [10] K. J. Satzinger, Y. P. Zhong, H.-S. Chang, G. A. Peairs, A. Bienfait, M.-H. Chou, A. Y. Cleland, C. R. Conner, . Dumur, J. Grebel, I. Gutierrez, B. H. November, R. G. Povey, S. J. Whiteley, D. D. Awschalom, D. I. Schuster, and A. N. Cleland, *Nature* **563**, 661 (2018).
- [11] L. B. Tan, O. Cotlet, A. Bergschneider, R. Schmidt, P. Back, Y. Shimazaki, M. Kroner, and A. mamolu, *Physical Review X* **10**, 021011 (2020), publisher: American Physical Society.
- [12] O. Cotlet, S. Zeytinoglu, M. Sigrist, E. Demler, and A. m. c. Imamoğlu, *Phys. Rev. B* **93**, 054510 (2016).
- [13] F. Schreck, L. Khaykovich, K. L. Corwin, G. Ferrari, T. Bourdel, J. Cubizolles, and C. Salomon, *Physical Review Letters* **87**, 080403 (2001), publisher: American Physical Society.
- [14] Z. Hadzibabic, C. A. Stan, K. Dieckmann, S. Gupta, M. W. Zwierlein, A. Grlitz, and W. Ketterle, *Physical Review Letters* **88**, 160401 (2002), publisher: American Physical Society.
- [15] A. A. Abrikosov, L. P. Gorkov, and I. E. Dzyaloshinski, *Methods of quantum field theory in statistical physics* (Courier Corporation, 2012).
- [16] J. M. Deutsch, *Reports on Progress in Physics* **81**, 082001 (2018).
- [17] L. D'Alessio, Y. Kafri, A. Polkovnikov, and M. Rigol, *Advances in Physics* **65**, 239 (2016), <https://doi.org/10.1080/00018732.2016.1198134>.
- [18] F. Borgonovi, F. Izrailev, L. Santos, and V. Zelevinsky, *Physics Reports* **626**, 1 (2016), quantum chaos and thermalization in isolated systems of interacting particles.
- [19] A. Smith, J. Knolle, D. L. Kovrizhin, and R. Moessner, *Phys. Rev. Lett.* **118**, 266601 (2017).
- [20] M. Brenes, M. Dalmonte, M. Heyl, and A. Scardicchio, *Phys. Rev. Lett.* **120**, 030601 (2018).

- [21] F. Piazza and P. Strack, *Physical Review A* **90**, 043823 (2014).
- [22] A. Chakraborty and F. Piazza, *Phys. Rev. Lett.* **127**, 177002 (2021).
- [23] F. Schlawin, A. Cavalleri, and D. Jaksch, *Physical Review Letters* **122**, 133602 (2019).
- [24] H. Gao, F. Schlawin, M. Buzzi, A. Cavalleri, and D. Jaksch, *Phys. Rev. Lett.* **125**, 053602 (2020).
- [25] E. Colella, M. L. Chiofalo, M. Barsanti, D. Rossini, and R. Citro, *Journal of Physics B: Atomic, Molecular and Optical Physics* **52**, 215301 (2019).
- [26] F. Schlawin and D. Jaksch, *Physical Review Letters* **123**, 133601 (2019).
- [27] A. Sheikhan and C. Kollath, *Phys. Rev. A* **99**, 053611 (2019).
- [28] M. A. Sentef, J. Li, F. Künzel, and M. Eckstein, *Physical Review Research* **2**, 033033 (2020).
- [29] J. Li and M. Eckstein, *Physical Review Letters* **125**, 217402 (2020), publisher: American Physical Society.
- [30] D. M. Kennes, E. Y. Wilner, D. R. Reichman, and A. J. Millis, *Nature Physics* **13**, 479 (2017).
- [31] A. Kamenev, *Field theory of non-equilibrium systems* (Cambridge University Press, 2011).
- [32] A. Chakraborty, P. Gorantla, and R. Sensarma, *Phys. Rev. B* **99**, 054306 (2019).
- [33] Let us point out that the definition of Γ in Eq.(28) is different from that in the standard thermal field theory where the external Fermion lines are full interacting Fermion Green's functions.
- [34] A. Chiochetta, D. Kiese, C. P. Zelle, F. Piazza, and S. Diehl, *Nature Communications* **12**, 5901 (2021).
- [35] C. Kittel, (2021).
- [36] C. Rylands, Y. Guo, B. L. Lev, J. Keeling, and V. Galitski, *Phys. Rev. Lett.* **125**, 010404 (2020).
- [37] B. Hacker, S. Welte, S. Daiss, A. Shaikat, S. Ritter, L. Li, and G. Rempe, *Nature Photonics* **13**, 110 (2019).
- [38] Lingenfelter Andrew, Roberts David, and Clerk A. A., *Science Advances* **7**, eabj1916, publisher: American Association for the Advancement of Science.
- [39] D. Hunger, S. Camerer, T. W. Hnsch, D. Knig, J. P. Kotthaus, J. Reichel, and P. Treutlein, *Physical Review Letters* **104**, 143002 (2010), publisher: American Physical Society.
- [40] H. Zhong, G. Flschner, A. Schwarz, R. Wiesendanger, P. Christoph, T. Wagner, A. Bick, C. Staarmann, B. Abeln, K. Sengstock, and C. Becker, *Review of Scientific Instruments* **88**, 023115 (2017), publisher: American Institute of Physics.
- [41] A. Altland and B. D. Simons, *Condensed matter field theory* (Cambridge University Press, 2010).
- [42] A. Klein, S. Lederer, D. Chowdhury, E. Berg, and A. Chubukov, *Phys. Rev. B* **97**, 155115 (2018).
- [43] F. Piazza and P. Strack, *Physical Review Letters* **112**, 143003 (2014).
- [44] J. Keeling, M. J. Bhaseen, and B. D. Simons, *Physical Review Letters* **112**, 143002 (2014).
- [45] Y. Chen, Z. Yu, and H. Zhai, *Physical Review Letters* **112**, 143004 (2014).
- [46] R. M. Sandner, W. Niedenzu, F. Piazza, and H. Ritsch, *EPL (Europhysics Letters)* **111**, 53001 (2015).
- [47] K. A. Fraser and F. Piazza, *Communications Physics* **2**, 48 (2019).
- [48] G. Mazza and A. Georges, *Physical Review Letters* **122**, 17401 (2019).
- [49] G. M. Andolina, F. M. D. Pellegrino, V. Giovannetti, A. H. MacDonald, and M. Polini, *Phys. Rev. B* **100**, 121109 (2019).
- [50] P. Nataf, T. Champel, G. Blatter, and D. M. Basko, *Phys. Rev. Lett.* **123**, 207402 (2019).
- [51] D. Guerci, P. Simon, and C. Mora, *Phys. Rev. Lett.* **125**, 257604 (2020).
- [52] F. Mivehvar, H. Ritsch, and F. Piazza, *Physical Review Letters* **122**, 113603 (2019).
- [53] J. Lang, D. E. Chang, and F. Piazza, *Physical Review A* **102**, 033720 (2020), publisher: American Physical Society.
- [54] J. Lang, D. Chang, and F. Piazza, *Physical Review Letters* **125**, 133604 (2020), publisher: American Physical Society.
- [55] T. Wasak, R. Schmidt, and F. Piazza, *Phys. Rev. Research* **3**, 013086 (2021).
- [56] T. Wasak, F. Pientka, and F. Piazza, arXiv preprint arXiv:2103.14040 (2021).